https://doi.org/10.1093/plcell/koac296 THE PLANT CELL 2023: 35: 369–389

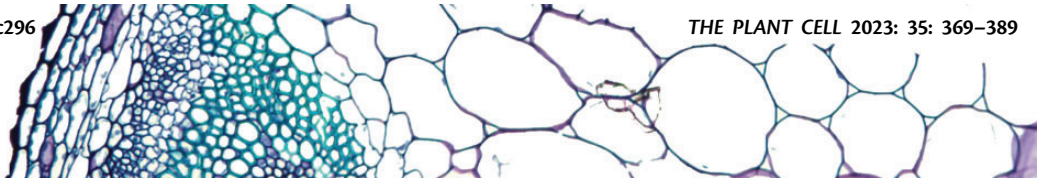

Research Article

The evening complex promotes maize flowering and adaptation to temperate regions

Yongping Zhao ,[1] Binbin Zhao ,[1] Yurong Xie ,[1,2] Hong Jia ,[3] Yongxiang Li ,[4] Miaoyun Xu ,[1,2] Guangxia Wu ,[1] Xiaojing Ma ,[1] Quanquan Li ,[1] Mei Hou ,[1] Changyu Li ,[1] Zhanchao Xia ,[1] Gang He ,[1] Hua Xu ,[1] Zhijing Bai ,[1] Dexin Kong ,[5] Zhigang Zheng ,[5] Qing Liu ,[5] Yuting Liu ,[5] Jinshun Zhong ,[5] Feng Tian ,[3] Baobao Wang [1,2,*] and Haiyang Wang [5,*]

1 Biotechnology Research Institute, Chinese Academy of Agricultural Sciences, Beijing, 100081, China
2 HainanYazhou Bay Seed Lab, Sanya, 572025, China
3 Department of Plant Genetics and Breeding, State Key Laboratory of Agrobiotechnology and National Maize Improvement Center, China Agricultural University, Beijing, 100193, China
4 Institute of Crop Science, Chinese Academy of Agricultural Sciences, Beijing, 10008, China
5 School of Life Sciences, and State Key Laboratory for Conservation and Utilization of Subtropical Agro-Bioresources, South China Agricultural University, Guangzhou, 510642, China

*Author for correspondence: whyang@scau.edu.cn (H.W.); wangbaobao@caas.cn (B.W.)
These authors contributed equally to this work (Y.Z., B.Z., and Y.X.)
H.W. and B.W. conceived and designed the project. Y.Z., B.Z., and Y.X. performed most of the experiments. M.X., H.X., Z.B., Q.Liu, Y.Liu, and J.Z. helped with some molecular experiments, G.W., Q.Li, Z.X., G.H., D.K., and Z.Z. conducted some field experiments and agronomic traits measurement. X.M. conducted Arabidopsis transformation and phenotypic analysis. M.H. and C.L. helped with bioinformatics analyses, Y.Li performed GWAS analysis of flowering time, and H.J. and F.T. analyzed the distribution of ZmELF3.1 genotypes in 1,008 accessions native to the Americas. H.W., Y.Z., B.W., and Y.X. wrote the manuscript.
The author responsible for distribution of materials integral to the findings presented in this article in accordance with the policy described in the Instructions for Authors (https://academic.oup.com/plcell) is: Haiyang Wang (whyang@scau.edu.cn).

Abstract

Maize (*Zea mays*) originated in southern Mexico and has spread over a wide latitudinal range. Maize expansion from tropical to temperate regions has necessitated a reduction of its photoperiod sensitivity. In this study, we cloned a quantitative trait locus (QTL) regulating flowering time in maize and show that the maize ortholog of *Arabidopsis thaliana EARLY FLOWERING3*, *ZmELF3.1*, is the causal locus. We demonstrate that ZmELF3.1 and ZmELF3.2 proteins can physically interact with ZmELF4.1/4.2 and ZmLUX1/2, to form evening complex(es; ECs) in the maize circadian clock. Loss-of-function mutants for *ZmELF3.1/3.2* and *ZmLUX1/2* exhibited delayed flowering under long-day and short-day conditions. We show that EC directly represses the expression of several flowering suppressor genes, such as the *CONSTANS, CONSTANS-LIKE, TOC1* (*CCT*) genes *ZmCCT9* and *ZmCCT10*, *ZmCONSTANS-LIKE 3*, and the *PSEUDORESPONSE REGULATOR* (*PRR*) genes *ZmPRR37a* and *ZmPRR73*, thus alleviating their inhibition, allowing florigen gene expression and promoting flowering. Further, we identify two closely linked retrotransposons located in the *ZmELF3.1* promoter that regulate the expression levels of *ZmELF3.1* and may have been positively selected during postdomestication spread of maize from tropical to temperate regions during the pre-Columbian era. These findings provide insights into circadian clock-mediated regulation of photoperiodic flowering in maize and new targets of genetic improvement for breeding.

Received January 24, 2022. Accepted September 16, 2022. Advance access publication September 29, 2022

Introduction

Maize (*Zea mays*) is a major staple crop worldwide, which by itself contributes ~40% of total cereal production (FAO, http://faostat.fao.org/). Although maize originated from its wild relative (teosinte) in southern Mexico about 9,000 years ago (Matsuoka et al., 2002), it has spread to temperate regions during pre-Columbian times, and is now cultivated across a wide latitudinal range (40°S to 45°N; Buckler et al., 2009). Nowadays, ~80% of the total worldwide maize production is produced in temperate regions (NCGA, 2021).

Flowering time is a key determinant of crop adaptation and yield productivity. As teosinte is a short-day (SD) plant, its flowering is accelerated under SD conditions, but delayed under long-day (LD) conditions. Thus, the spread of maize from tropical to temperate regions has necessitated a reduction of its photoperiod sensitivity for adaptation to LD conditions (Hung et al., 2012). A number of genes that contributed to the pre-Columbian expansion of maize to temperate regions have been cloned and functionally characterized, including a *Flowering Locus T* (*FT*) homolog, *CENTRORADIALIS 8* (*ZCN8*) (Lazakis et al., 2011; Meng et al., 2011; Guo et al., 2018), *Vgt1* (encoding an APETALA 2-like transcription factor) (Salvi et al., 2007; Ducrocq et al., 2008; Castelletti et al., 2014), *ZmCCT* (*CONSTANS, CONSTANS-LIKE, TOC1*; also named *ZmCCT10*) (Hung et al., 2012; Yang et al., 2013), *ZmCCT9* (Huang et al., 2018), *ZmMADS69* (Liang et al., 2018), *Delayed flowering 1* (which encodes a basic leucine zipper transcription factor that physically interacts with ZCN8) and *ZmMADS67* (Sun et al., 2020). Independently, genomic studies with nested association mapping (NAM) populations and diverse association panels have identified hundreds of candidate genes with small effects that may contribute to large-scale environmental adaptation of maize to altitude and latitude, such as *DWARF8*, *Phytochrome C2* (*ZmPHYC2*), *CIRCADIAN CLOCK ASSOCIATED 1* (*ZmCCA1*), *Zea Floricaula/Leafy 1/2*, *Zea mays MADS-box 5* (*ZMM5*), *Barren inflorescence 2*, *EARLY FLOWERING 3* (*ZmELF3*), *PSEUDORESPONSE REGULATOR 37* (*ZmPRR37*), and *ZmPRR73*, to name a few (Thornsberry et al., 2001; Chardon et al., 2004; Salvi et al., 2007; Buckler et al., 2009; Hung et al., 2012; Bouchet et al., 2013; Li et al., 2016; Romero Navarro et al., 2017; Li et al., 2020). However, for most, functional validation on flowering regulation, evaluation of their allelic effects on regional adaptation, and identification of the causal variants remain to be carried out.

The evening complex (EC) was first identified in Arabidopsis (*Arabidopsis thaliana*); it is composed of three interacting proteins, ELF3, ELF4, and LUX ARRHYTHMO (LUX). ELF3 directly interacts with and bridges ELF4 and LUX to form a transcriptional repressor complex and a core component of the plant circadian clock (Nusinow et al., 2011). LUX is a single MYB domain-containing SHAQYF-type GARP transcription factor that can mediate the direct binding of the EC to the specific LUX-binding site (LBS) motif 5′-GATWCG-3′ (where W indicates A or T) in target promoters (Nusinow et al., 2011). Mutations in any of the three genes result in early flowering under SD and LD conditions and elongated hypocotyls, and thus they were believed to mediate circadian clock regulation of photoperiod-mediated flowering in Arabidopsis (Hicks et al., 1996; Zagotta et al., 1996; Doyle et al., 2002; Hazen et al., 2005). Recent studies have shown that the EC plays a conserved role in regulating photoperiod sensitivity and regional adaptation in various crops. For example, the *ELF3* orthologs in rice (*Oryza sativa*) *OsELF3.1* (also named *Early heading 7* and *Heading date 17*; Matsubara et al., 2012; Saito et al., 2012; Zhao et al., 2012; Zhu et al., 2018), *HIGH RESPONSE TO PHOTOPERIOD* of pea (*Pisum sativum*; Weller et al., 2012), *EARLY MATURITY 8* of barley (*Sorghum vulgare*; Faure et al., 2012; Zakhrabekova et al., 2012), and the soybean (*Glycine max*) *J* gene (Lu et al., 2017) are important targets of postdomestication breeding selection for regional adaptation of various crops. In addition, LUX orthologs in several crops (barley, einkorn wheat [*Triticum monococcum*], pea, and soybean) have also been shown to regulate photoperiodic flowering and regional adaptation (Mizuno et al., 2012; Campoli et al., 2013; Liew et al., 2014; Bu et al., 2021).

In this study, we report the cloning of a QTL regulating flowering time in maize and show that an ortholog of Arabidopsis *ELF3*, *ZmELF3.1*, corresponds to this QTL. We demonstrate that *ZmELF3.1* and its homolog *ZmELF3.2* exhibit canonical diurnal pattern of expression, and their protein products exclusively localized to the nucleus. We show that both ZmELF3.1 and ZmELF3.2 can physically interact with two maize homologs of Arabidopsis ELF4, namely ZmELF4.1 and ZmELF4.2, and two maize homologs of Arabidopsis LUX, ZmLUX1, and ZmLUX2, thus constituting the maize EC. Loss-of-function mutants of *ZmELF3*s and *ZmLUX*s exhibit a significant delay in flowering time under both LD and SD conditions, with ZmELF3.1 and ZmLUX1 playing a more predominant role. We further demonstrate that the EC can repress the expression of several known flowering suppressor genes, *ZmCCT9*, *ZmCCT10*, *ZmCOL3*, *ZmPRR37a*, and *ZmPRR73*, in turn, alleviating their inhibition of the expression of several maize florigen genes (*ZCN8*, *ZCN7*, and *ZCN12*) to promote flowering. Finally, we identified two closely linked variants (a NonLTR/*L1* retrotransposon and an LTR/*Gypsy* retrotransposon) inserted upstream of the *ZmELF3.1* coding region that regulate *ZmELF3.1* expression, and that they have been positively selected during the spread of maize from tropical to temperate regions for adaptation to higher latitudes.

Results

Identification of *ZmELF3.1* as a candidate QTL for flowering time and photoperiod sensitivity

To identify new factor(s) having contributed to regional expansion of maize, we reanalyzed flowering time and photoperiod-sensitive QTLs previously identified in the maize NAM population (Buckler et al., 2009; Hung et al., 2012; Li et al., 2016). We repeatedly identified a significant QTL located at the end of chromosome 3 (216.5–221.5 Mb,

centered at ~218.4 Mb, based on the B73_v2 reference genome, thus named *qFT3_218*) in different NAM families (different founder lines crossed to B73), with nine families detected for days to anthesis (DTA), six families for days to silking (DTS), six families for anthesis photoperiod response, and five families for silking photoperiod response. Notably, we mostly detected this QTL in families derived from tropical founder lines crossed to B73 (a temperate inbred line) (Figure 1A). These observations indicate that *qFT3_218* likely encompasses a genetic element(s) involved in the expansion of maize from tropical to temperate regions.

To identify the possible candidate gene(s) underlying *qFT3_218*, we re-performed a genome-wide association study (GWAS) for flowering time of all NAM recombinant inbred lines (RILs) using the phenotypic data across 13 environments (Buckler et al., 2009; Li et al., 2016; Figure 1B). We detected a significant signal around 218.8 Mb (B73_v2) for DTA (*P*-value = 1.48e−7) and DTS (*P*-value = 7.84e−7), with the peak single-nucleotide polymorphism (SNP; S3_218895116) being located 2.5 kb downstream of a gene (GRMZM2G045275, chromosome 3: 218,897,671–218,903,527 bp, reverse strand, B73_v2, corresponding to Zm00001d044232 in the B73_v4 genome) encoding a protein homologous to Arabidopsis ELF3 (27.9% amino acid identity). As *ELF3* orthologs have been shown to regulate flowering time and photoperiod sensitivity in Arabidopsis and a number of crops, we speculated that GRMZM2G045275 (Zm00001d044232) probably represents the candidate gene for *qFT3_218*.

ZmELF3s form ECs with ZmELF4s and ZmLUXs

In Arabidopsis, ELF3 physically interacts with both ELF4 and LUX to form the EC, in which LUX is the transcription factor that regulates downstream gene expression (Nusinow et al., 2011; Chow et al., 2012). BLAST searches identified a gene (Zm00001d039156) highly homologous to the ELF3-like protein encoded by the *qFT3_218* candidate locus GRMZM2G045275 (Zm00001d044232; 42.9% amino acid identity) in the maize B73_v4 genome. Thus, we designated these two genes *ZmELF3.1* (Zm00001d044232, candidate for *qFT3_218*) and *ZmELF3.2* (Zm00001d039156) (Supplemental Figure S1). In addition, we identified two genes homologous to Arabidopsis *ELF4*, designated *ZmELF4.1* and *ZmELF4.2*, with 35.65% and 30.1% amino acid identity to Arabidopsis *ELF4*, respectively (Supplemental Figure S2). We also detected four homologs of Arabidopsis *LUX*, designated *ZmLUX1*, *ZmLUX2*, *ZmLUX3*, and *ZmLUX4*, whose encoding proteins showed 42.1%, 46.8%, 34.2%, and 32.9% amino acid identity with Arabidopsis LUX, respectively (Supplemental Figure S2). Interestingly, both ZmELF3.1 and ZmELF3.2 lack the polyglutamine (polyQ) repeats and the C-terminal prion-like domain (PrD) (Lancaster et al. 2014), which have been shown to play important roles in thermomorphogenesis for Arabidopsis ELF3 (Undurraga et al., 2012; Jung et al., 2020; Supplemental Figure S1). Yeast two-hybrid (Y2H) (Figure 1C), bimolecular fluorescence complementation (BiFC) (Figure 1D) and luciferase complementation imaging (LCI) (Figure 1E) assays all confirmed that both ZmELF3.1 and ZmELF3.2 physically interact with ZmELF4.1/4.2 and ZmLUX1/2, but we observed no direct interaction between ZmELF4.1/4.2 and ZmLUX1/2. Moreover, a yeast three-hybrid assay indicated that ZmELF3.1/3.2 bridge the interaction between ZmELF4.1/ZmELF4.2 and ZmLUX1/2 to form EC (Figure 1F), supporting the existence of conserved EC in maize. Reverse transcription-quantitative PCR (RT-qPCR) assays also showed that these genes all display distinct diurnal expression patterns under both LD and SD conditions, with *ZmELF3.1*, *ZmELF4.1*, and *ZmLUX1* showing obviously higher expression levels than their respective homologs (Figure 2, A–F). Protein subcellular localization assay also showed that their green fluorescent protein (GFP) fusion proteins were all exclusively localized to the nucleus (Figure 2G).

Delayed flowering of the *Zmelf3* and *Zmlux* mutants under both LD and SD conditions

To investigate the function of maize EC components in regulating flowering time, we first overexpressed *ZmELF3* genes in the Arabidopsis *elf3-7* mutant. We determined that both *ZmELF3.1* and *ZmELF3.2* can rescue the Arabidopsis *elf3-7* mutant phenotype, including long-hypocotyl and early flowering under LD conditions (Supplemental Figure S3), when overexpressed, indicating a conserved biological role of ZmELF3s in regulating flowering. We also generated both single and double knockout (*ko*) mutants in *ZmELF3*s using clustered regularly interspaced short palindromic repeats (CRISPR)/CRISPR-associated nuclease 9 (Cas9)-mediated gene editing (Supplemental Figure S4). We selected three independent *Zmelf3.1* single mutants (ko1#–ko#3), three independent *Zmelf3.2* single mutants (ko#4–ko#6), and three independent *Zmelf3.1 Zmelf3.2* double mutants (ko#7–ko#9) (Supplemental Figure S4) for analyses. We sowed all mutants together with their respective wild-type (WT) in fields at Langfang (39.53° N/116.72° E, LD) and Sanya (18.73° N/109.17° E, SD) for phenotypic examination. These field tests showed that the *Zmelf3.1* single mutants, but not the *Zmelf3.2* single mutants, flower significantly later than the WT plants under both LD and SD conditions (8–12 days late in anthesis and 9–15 days late in silking). Moreover, the *Zmelf3.1 Zmelf3.2* double mutants flowered significantly later than the *Zmelf3.1* single mutants, suggesting that ZmELF3.1 and ZmELF3.2 likely play partially redundant functions in flowering regulation, with ZmELF3.1 playing a predominant role (Figure 3, A–D). Both the *Zmelf3.1* single mutants and *Zmelf3.1 Zmelf3.2* double mutants displayed a more pronounced delay in flowering time under LD conditions than under SD conditions (the *Zmelf3.1* single mutants delayed flowering by ~3.8 more days under LD than under SD, and the *Zmelf3.1 Zmelf3.2* double mutants by ~4 more days under LD than under SD conditions), indicating that ZmELF3.1/ZmELF3.2 likely play a more important role in promoting flowering under LD conditions. Consistently, the *Zmelf3.1* single mutants and the *Zmelf3.1 Zmelf3.2* double mutants, but not the *Zmelf3.2* single mutants, displayed

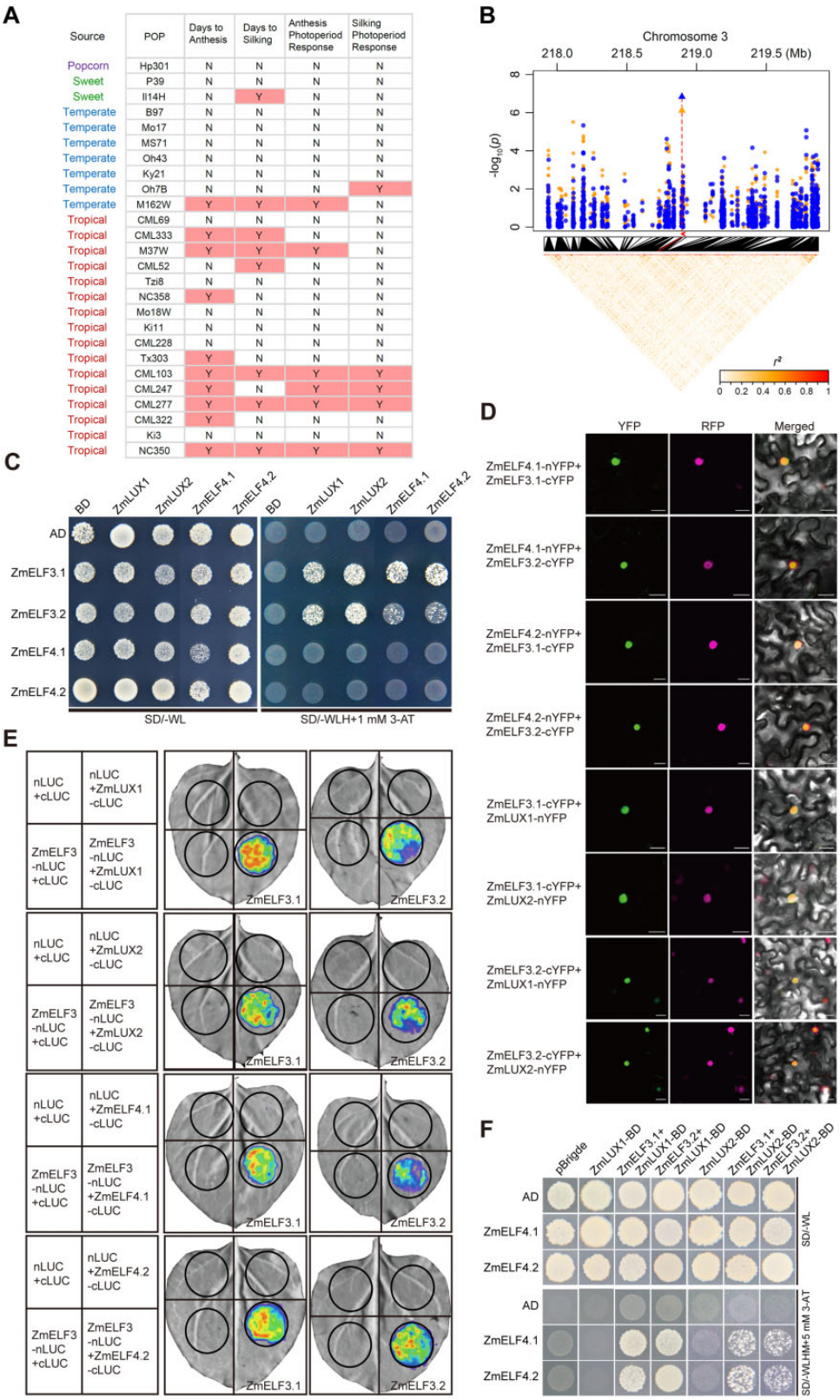

Figure 1 ZmELF3s bridge ZmELF4s and ZmLUXs to form the EC. A, Linkage mapping using the NAM population identifies a QTL for flowering time and photoperiod response around the *ZmELF3.1* region. Y or N, with or without QTL detected around the *ZmELF3.1* region. B, GWAS identification of *ZmELF3.1* as a candidate gene for variation in the traits DTA and DTS. The candidate genes for DTA and DTS are marked with blue points and orange points, respectively. Peak markers are shown as triangles for each trait and their positions in the linkage disequilibrium heatmap are indicated by red lines. The position of the candidate gene in the Manhattan plot is shown by the red arrow. C, Y2H assay showing that ZmELF3.1/3.2 directly interact with both ZmELF4.1/4.2 and ZmLUX1/2. Three independent experiments showed similar results. D, BiFC assay showing that ZmELF3.1/3.2 directly interact with both ZmELF4.1/4.2 and ZmLUX1/2 in *N. benthamiana* leaf cells. The *AHL22-ERFP* marker was co-

(continued)

higher plant height and ear height, and increased leaf number, under both LD and SD conditions, compared to the WT control plants (Supplemental Figure S4). Consistent with the delayed flowering phenotype of the *Zmelf3.1 Zmelf3.2* double mutants, RT-qPCR analysis showed that the expression of three reported maize florigen genes (*ZCN8*, *ZCN7*, and *ZCN12*) (Meng et al., 2011; Castelletti et al., 2014; Mascheretti et al., 2015) is nearly not detectable in the *Zmelf3.1 Zmelf3.2* double mutant under both SD and LD conditions (Figure 3, E–J).

We also generated CRISPR/Cas9-aided *ko* mutants for *ZmLUX1/2* (Supplemental Figure S5). We determined that the *Zmlux1* and *Zmlux2* single mutants and the *Zmlux1 Zmlux2* double mutants all showed obviously delayed flowering under both SD and LD conditions, compared to the WT control (Figure 3, K–N). Moreover, the *Zmlux1 Zmlux2* double mutants flowered significantly later than the *Zmlux1* or *Zmlux2* single mutants, suggesting that ZmLUX1 and ZmLUX2 also play partially redundant functions in flowering regulation (Figures 3, K–N). These results support the notion that the EC contributes to promoting flowering in maize. However, we observed no significant differences in flowering time between the *ZmELF3.1* overexpressors and WT plants (Supplemental Figure S6), suggesting that the functional levels of the EC components might be optimal in WT plants. A similar observation was reported for the *LUX1* and *LUX2* genes in soybean (Bu et al., 2021).

ZmLUX1 directly represses the expression of a group of flowering repressor genes

Previous studies have reported that the Arabidopsis EC directly regulates the expression of clock-regulated genes (such as *PHYTOCHROME-INTERACTING FACTOR 4* [*PIF4*], *PIF5*, and *PRR9*) to optimize plant growth and flowering time (Nakamichi et al., 2005; Nusinow et al., 2011; Chow et al., 2012). We thus tested whether the maize EC directly regulates the expression of a set of flowering repressor genes (*ZmCCT10*, *ZmCCT9*, *CONSTANS-LIKE 3* [*ZmCOL3*], *ZmPRR37a*, and *ZmPRR73*) (Hung et al., 2012; Li et al., 2016; Huang et al., 2018; Jin et al., 2018) by RT-qPCR. We observed that the expression of these flowering repressor genes significantly increases in the *Zmelf3.1 Zmelf3.2* double mutants, compared to the WT plants (Figure 4A; Supplemental Figure S7). Sequence analysis revealed that their promoters all contain multiple copies of the LUX binding site (GATWCG; Nusinow et al., 2011; Lu et al., 2017; Figure 4B), raising the possibility that the maize EC directly regulates their expression. A yeast one-hybrid (Y1H) assay showed that indeed, ZmLUX1 binds strongly to specific promoter fragments of *ZmPRR37a*, *ZmPRR73*, *ZmCOL3*, and *ZmCCT9*, but only weakly to the promoter fragments of *ZmCCT10* (Figures 4, C and D; Supplemental Figure S8). We verified the binding of ZmLUX1 to the *ZmPRR37a* promoter by electrophoretic mobility shift assay (EMSA) (Figure 4E). Further, we performed chromatin immunoprecipitation (ChIP)-qPCR assay using the leaves from V2-stage *ZmELF3.1* overexpressing plants (ELF3.1 being tagged with the GFP) with an anti-GFP antibody. We again detected the binding of ZmELF3.1 to the promoter fragments of *ZmPRR37a*, *ZmPRR73*, *ZmCOL3*, and *ZmCCT9 in vivo* (Figure 4F). A transient expression assay in *Nicotiana bentamiana* leaf epidermal cells further showed that the transcription of *ZmCCT9*, *ZmCOL3*, *ZmPRR37a*, *ZmPRR73*, and *ZmCCT10* (as measured by promoter constructs where each promoter individually drives firefly luciferase [*LUC*] expression) is significantly repressed upon co-expression of *YFPn-ZmLUX1*, *YFPn-ZmLUX2*, *YFPc-ZmELF3.1*, *YFPc-ZmELF3.2*, *YFPn-ZmELF4.1*, or *YFPn-ZmELF4.2*, compared to the control vector (p2YN [YFPn] or p2YC [YFPc]) (Figure 4, G and H), suggesting that the three components of the EC (ZmELF3s, ZmELF4s, and ZmLUXs) act together to repress the expression of downstream flowering genes.

ZmCOL3 was previously shown to act as a flowering repressor by directly activating the transcription of *ZmCCT10*, which in turn represses the expression of *ZCN8* (Jin et al., 2018). Thus, we tested the effects of ZmCCT9, ZmCOL3, ZmPRR37a, and ZmPRR73 on downstream florigen gene expression. To this end, we transiently expressed *ZmCCT9*, *ZmCOL3*, *ZmPRR37a*, or *ZmPRR73* in *N. benthamiana* leaf epidermal cells together with *promoter:LUC* reporter constructs. In all cases, the expression of *ZCN8*, *ZCN7*, or *ZCN12* repressed the transcriptional output of the *ZCN7*, *ZCN8*, and *ZCN12* promoters (Figure 4I). Together, these results support the notion that the maize EC promotes flowering through suppressing the expression of a set of flowering repressor genes (*ZmCCT9*, *ZmCCT10*, *ZmCOL3*, *ZmPRR37a*, and *ZmPRR73*).

Insertion of two retrotransposons upstream of *ZmELF3.1* confers increased expression and early flowering

To investigate whether and how natural variation of *ZmELF3.1* influences maize flowering time, we took advantage of the recently released high-quality genome assembly of 45 maize inbred lines, comprising B73 (Jiao et al., 2017), Mo17 (Sun et al., 2018), W22 (Springer et al., 2018), 4

Figure 1 (Continued)
infiltrated to indicate the nuclei. The interaction between nYFP and ZmELF3-cYFP or between cYFP and ZmELF4-nYFP (or ZmLUX-nYFP) is shown in Supplemental Figure S3C as the negative controls. Scale bar, 20 μm. Three independent experiments were performed, with similar results. E, LCI assay demonstrating the interaction between ZmELF3.1/3.2 with ZmELF4.1/4.2 or ZmLUX1/2 in *N. benthamiana* leaves. Three independent experiments were performed, with similar results. Representative images of *N. benthamiana* leaves 72 h after infiltration are shown. F, Yeast three-hybrid assay showing that ZmELF3.1/3.2, ZmELF4.1/4.2 and ZmLUX1/2 interact to form a tri-protein complex(es) in yeast. Two independent experiments showed similar results.

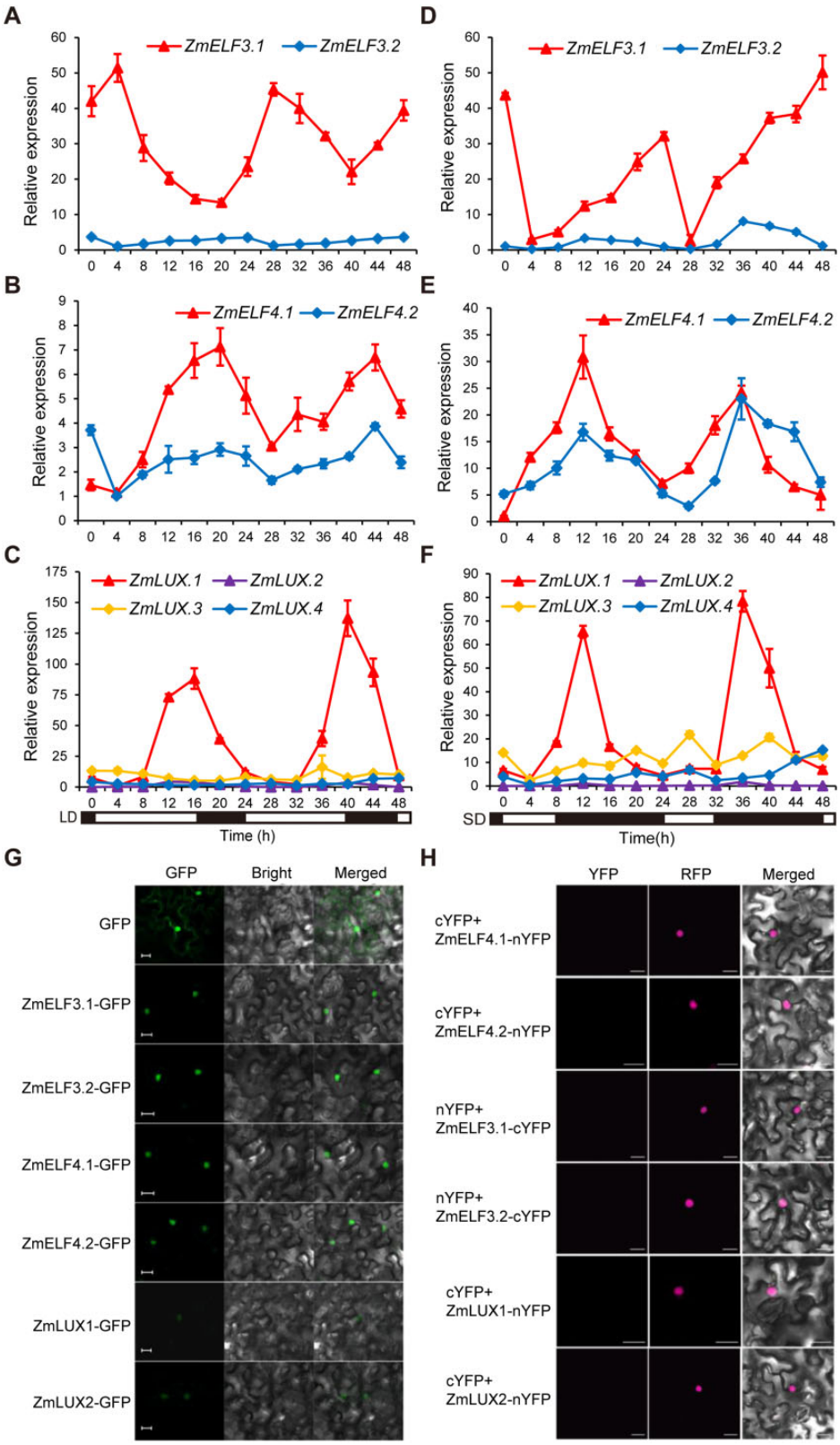

Figure 2 Expression pattern of *ZmELF3*s, *ZmELF4*s, and *ZmLUX*s and subcellular localization of their encoded proteins. A–F, *ZmELF3.1/3.2*, *ZmELF4.1/4.2*, and *ZmLUX1/2/3/4* all show a rhythmic diurnal expression pattern under both LD (A–C) and SD (D–F) conditions. The sixth leaves from V6-stage plants of ZC01 (a temperate line) grown under the indicated conditions were used for RNA extraction and RT-qPCR. Values are means ± SD (n = 3 technical replicates). Two independent experiments were performed and the results were similar (leaves from six different plants were used for each biological replicate). The black bars and white bars indicate the dark period and the light period, respectively. G, ZmELF3.1/3.2, ZmELF4.1/4.2, and ZmLUX1/2 proteins localize to the nucleus. The expression constructs *GFP*, *ZmELF3.1/3.2-GFP*, *ZmELF4.1/4.2-GFP*,

(continued)

European maize lines (Haberer et al., 2020), 26 founder lines of the NAM population (Hufford et al., 2021), and 12 founder inbred lines for modern temperate maize breeding (Wang et al., 2022; Supplemental Data Set S1). We analyzed both the *ZmELF3.1* coding regions and its flanking regions up to the next neighboring gene on either side. We detected only a few nonsynonymous mutations in the coding sequences of eighty tropical inbred lines and eighty temperate inbred lines (Supplemental Data Set S2), suggesting that variation in the regulatory regions of *ZmELF3.1* might play a predominant role in regulating its function. Notably, sequencing analysis identified two retrotransposon insertions: a Nonlong terminal repeat (NonLTR)/*L1*-type retrotransposon (6.5 kb in length) and an LTR/*Gypsy* type retrotransposon (11.8 kb in length), located 7 and 31 kb upstream of the *ZmELF3.1* translational start site, respectively, in 22 maize inbred lines (including B73), but not another 23 inbred lines (like Ki3) (Figure 5A; Supplemental Figure S9). As structural variation in regulatory regions often influences transcription and flowering time in maize, we speculated that these retrotransposons may affect *ZmELF3.1* expression, and thus flowering time. Consistent with this notion, nine NAM founder lines carrying the retrotransposon insertions flowered earlier (∼9–10 d) showed higher *ZmELF3.1* expression than another 18 founder lines that lacked the retrotransposon insertions (Figure 5, B and C). Moreover, in contrast to B73 (a temperate inbred line), most families of the NAM population in which we detected *qFT3_218* for DTA (all 9), DTS (5 of 6), anthesis photoperiod response (all 10) and silking photoperiod response (11 of 12) (Buckler et al., 2009; Hung et al., 2012; Li et al., 2016), their founder lines all lacked the retrotransposon insertions upstream of their *ZmELF3.1* genes (except I114H for DTS, and Oh7B for silking photoperiod response) (Supplemental Data Set S3). These observations indicate that the retrotransposon insertions likely contribute to the differential expression and photoperiod flowering in the NAM founder lines.

To further test the effect of these two retrotransposons, we genotyped and phenotyped 415 maize inbred lines from a natural association population (Yang et al., 2014). Among them, 272 lines carried both retrotransposons while the remaining 143 lines lacked both retrotransposons (Supplemental Data Set S3), suggesting that these two retrotransposons are tightly linked. In addition, the inbred lines with the retrotransposon insertions flowered on average earlier than the inbred lines without the retrotransposon insertions under both LD (Langfang in 2015) and SD (Sanya in 2016) conditions. Notably, the differences in DTA were larger in tropical lines with and without the retrotransposon insertions than in temperate lines with and without the retrotransposon insertions, and the difference in DTA was larger under LD conditions, compared to SD conditions (Figure 5, D and E). Moreover, RT-qPCR analysis showed that three randomly selected inbred lines with the retrotransposon insertions (B73, W138, and GY237) all exhibit higher expression levels of *ZmELF3.1* than three randomly selected inbred lines that do not carry the insertion (CIMBL1, CIMBL26, and CIMBL32) (Figure 5F). Consistently, the inbred lines with the retrotransposon insertions (B73, W138, and GY237) had lower expression of the EC target genes (*ZmCCT9*, *ZmPRR37a*, *ZmPRR73*, and *ZmCOL3*) than the inbred lines that do not carry the insertion (CIMBL1, CIMBL26, and CIMBL32) (Supplemental Figure S10). Collectively, these observations suggest that the two-tightly linked retrotransposons likely represent the causal variation underlying the differential expression of *ZmELF3.1*, and thus flowering time.

To validate this hypothesis, we cloned the B73 and Ki3 *ZmELF3.1* promoter sequences that differ only at the two retrotransposons into a reporter construct upstream of a minimal promoter from the cauliflower mosaic virus (MIN35S), the *LUC* sequence and the CaMV poly(A) terminator (Figure 5G) for transient expression assays in *N. benthamiana* leaves. We established that the B73 construct containing the LTR/*Gypsy* element drastically enhances luciferase activity (∼14-fold), while the B73 construct containing the NonLTR/*L1* element markedly represses luciferase activity (approximately 3-fold), relative to the control Ki3 construct with no insertions (Figure 5, H–J). These results suggest that in combination, the LTR/*Gypsy* and NonLTR1/*L1* elements likely act to promote *ZmELF3.1* transcription, which is consistent with the observed higher expression of *ZmELF3.1* in inbred lines with the retrotransposon insertions (Figure 5, C and F).

The retrotransposon insertions were positively selected during postdomestication of maize and contributed to adaptation of maize to temperate regions

To examine the evolutionary origin of the LTR/*Gypsy* element, we genotyped the LTR/*Gypsy* and NonLTR1/*L1* elements in 72 teosinte accessions (Supplemental Data Set S4). Interestingly, two accessions carried both the LTR/*Gypsy* and NonLTR1/*L1* elements (Supplemental Figure S11), indicating that the LTR/*Gypsy* and NonLTR1/*L1* retrotransposon insertions were already present in the maize ancestor. To determine whether selection has acted on the LTR/*Gypsy* and NonLTR/*L1* elements during the pre-Columbian expansion of maize, we analyzed nucleotide diversity (π) and Tajima's *D* across a 90-kb region centered on *ZmELF3.1* in the 45

Figure 2 (Continued)
and *ZmLUX1/2-GFP* were individually infiltrated into *N. benthamiana* leaves and then incubated for 48 h in the dark prior to imaging using a confocal microscope. Scale bars, 20 μm. Three independent experiments were performed, with similar results. H, Negative controls for the BiFC assay for the interaction between ZmELF3.1/3.2, ZmELF4.1/4.2, and ZmLUX1/2 proteins. The nuclear marker *AHL-RFP* indicates the nuclei in *N. benthamiana* leaf epidermal cells. Scale bars, 20 μm. Three independent experiments were performed, with similar results.

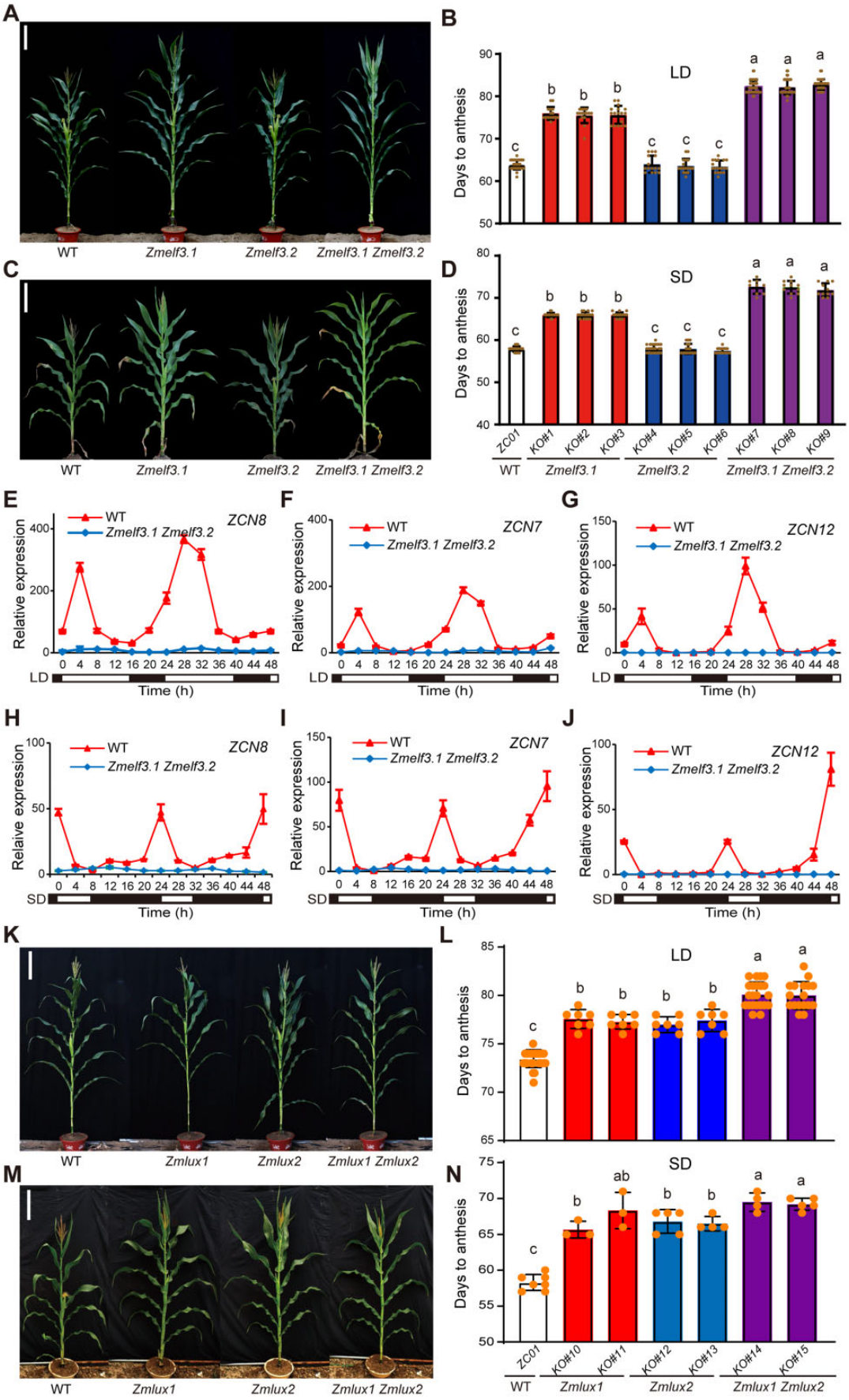

Figure 3 Maize EC regulates flowering time under both LD and SD conditions. A–D, Comparison and quantification of the flowering time of WT, *Zmelf3.1* and *Zmelf3.2* single mutants, and the *Zmelf3.1 Zmelf3.2* double mutant under LD (A, B) or SD (C, D) conditions. Scale bars, 30 cm. Values

(continued)

maize inbred lines (27 temperate, 18 tropical) with high-quality genome assemblies (Supplemental Data Set S1). Notably, in the region of the LTR/*Gypsy* and NonLTR/*L1* elements, the nucleotide diversity (π) in temperate maize was much lower than that in tropical maize. Tajima's *D* values of temperate maize were about −1.6 and −2.4, but Tajima's *D* values of tropical maize were 1.2 and 2.0 (Supplemental Figure S11). These data indicate a strong positive selection on the LTR/*Gypsy* and NonLTR/*L1* elements. On the contrary, we detected no significant selection signals over the *ZmELF3.1* coding region.

To investigate whether these two retrotransposons contributed to the expansion and adaptation of maize to temperate regions, we analyzed their distribution in 72 accessions of teosinte, 415 of a panel of 513 maize inbred lines with 196 tropical inbred lines and 219 temperate inbred lines (Yang et al., 2014; Supplemental Data Sets S3 and S4) and 327 of the 350 modern temperate maize inbred lines (Wang et al., 2020; Supplemental Data Set S5). We determined that 2.8% of teosinte, 7.7% of tropical inbred lines, 58.4% of temperate inbred lines, and 74.6% of modern maize inbred lines carry the two retrotransposons (Figure 6A), suggesting that these two retrotransposons have likely been selected during the expansion of maize from tropical to temperate regions and are still under continuous selection during modern temperate maize breeding. To substantiate this notion, we investigated the distribution of the LTR/*Gypsy* retrotransposon among 1,008 maize landrace accessions representing the entire pre-Columbian range of maize races native to the Americas (Huang et al., 2018; Supplemental Data Set S6). Strikingly, the LTR/*Gypsy* retrotransposon showed strong association with latitude, predominantly accumulating in landraces of higher latitudes. In contrast, the maize landraces without the LTR/*Gypsy* retrotransposon were mainly distributed at low latitudes (Figure 6, B–D).

Discussion

The circadian clock is an internal time-keeping mechanism that enables plants to anticipate changes in external environmental conditions (such as dawn, dusk, and changes in temperature driven by daily light/dark cycles) and adjust their development and physiology accordingly (Hsu and Harmer, 2014). One major output of the circadian clock is flowering time, which is a critical determinant of regional adaptation for plants. Recent studies have demonstrated that the EC plays a conserved role in regulating photoperiod flowering in both SD and LD plants, and thus, its components have often been targets of artificial selection for crop domestication and improvement (Liu et al., 2020; McClung, 2021). For example, orthologs of *ELF3* in rice, pea, barley, wheat, and soybean (Faure et al., 2012; Matsubara et al., 2012; Weller et al., 2012; Zakhrabekova et al., 2012; Lu et al., 2017; Zhu et al., 2018), orthologs of *LUX* in barley, einkorn wheat, pea, soybean, and rice (Mizuno et al., 2012; Campoli et al., 2013; Liew et al., 2014; Bu et al., 2021; Cai et al., 2022), orthologs of *PRR7* in sugar beet (*Beta vulgaris*), rice, barley, wheat, sorghum, and soybean (Murakami et al., 2005; Turner et al., 2005; Beales et al., 2007; Murphy et al., 2011; Pin et al., 2012; Bu et al., 2021; Liang et al., 2021) regulate photoperiodic flowering and regional adaptation of various crops.

In this study, we showed that *ZmELF3.1* corresponds to *qFT3_218*, a QTL regulating flowering time in maize. In addition, we established that the expression of *ZmELF3.1/3.2*, *ZmELF4.1/4.2*, and *ZmLUX1/2* follows a diurnal rhythm and that ZmELF3.1/3.2 can physically interact with ZmELF4.1/4.2 and ZmLUX1/2, to form the ECs of the maize circadian clock. Similar to other SD plants with defective EC (like rice and soybean), loss-of-function mutants of *ZmELF3.1/3.2* and *ZmLUX1/2* exhibited delayed flowering time under both LD and SD conditions. Moreover, overexpression of either *ZmELF3.1* or *ZmELF3.2* largely rescued the long-hypocotyl and early flowering phenotypes of the Arabidopsis *elf3-7* mutant (Supplemental Figure S3). These observations indicate that ZmELF3.1/3.2 and the EC play a conserved role in regulating flowering time in maize.

At the mechanistic level, previous studies have shown that the EC mainly acts as a transcriptional repressor to suppress the expression of downstream flowering regulatory genes. For example, in rice (an SD plant), an ortholog of *ELF3* (*OsELF3-1*) negatively regulates the expression of the major flowering repressor *Grain number, plant height, and heading date7* (an ortholog of Arabidopsis *PRR7*), and consequently upregulates the expression of the downstream genes *Ehd1* and *FT*-like to promote flowering under both SD and LD conditions (Saito et al., 2012; Zhao et al., 2012). In soybean (an SD plant), the EC suppresses the transcription of a key flowering repressor, the legume-specific *E1* gene (which encodes a B3 superfamily member), thereby relieving the suppression of *FT2a* and *FT5a* imposed by E1, and promoting flowering (Lu et al., 2017; Bu et al., 2021). In Arabidopsis (an LD plant), ELF3 can be recruited to the *PRR9* promoter through LUX to repress *PRR9* expression, thus delaying

Figure 3 (Continued)
are means ± SD ($n \geq 11$ plants). Different lowercase letters indicate significant differences determined by the Duncan's multiple-range test ($P < 0.05$). E–J, The relative transcript levels of three maize florigen genes (*ZCN8*, *ZCN7*, and *ZCN12*) are downregulated in the *Zmelf3.1 Zmelf3.2* double mutant grown under LD (E–G) or SD (H–J) conditions. Leaves from V6-stage plants grown under the indicated conditions were harvested for RNA extraction. Values are means ± SD ($n = 3$ biological replicates). Two independent experiments were performed, with similar results. K–N, Comparison and quantification of the flowering time of WT, *Zmlux1*, and *Zmlux2* single mutants and the *Zmlux1 Zmlux2* double mutant grown under LD (K, L) or SD (M, N) conditions. Scale bars, 30 cm. Values are means ± SD ($n \geq 3$ plants). Different lowercase letters indicate significant differences determined by Duncan's multiple-range test ($P < 0.05$).

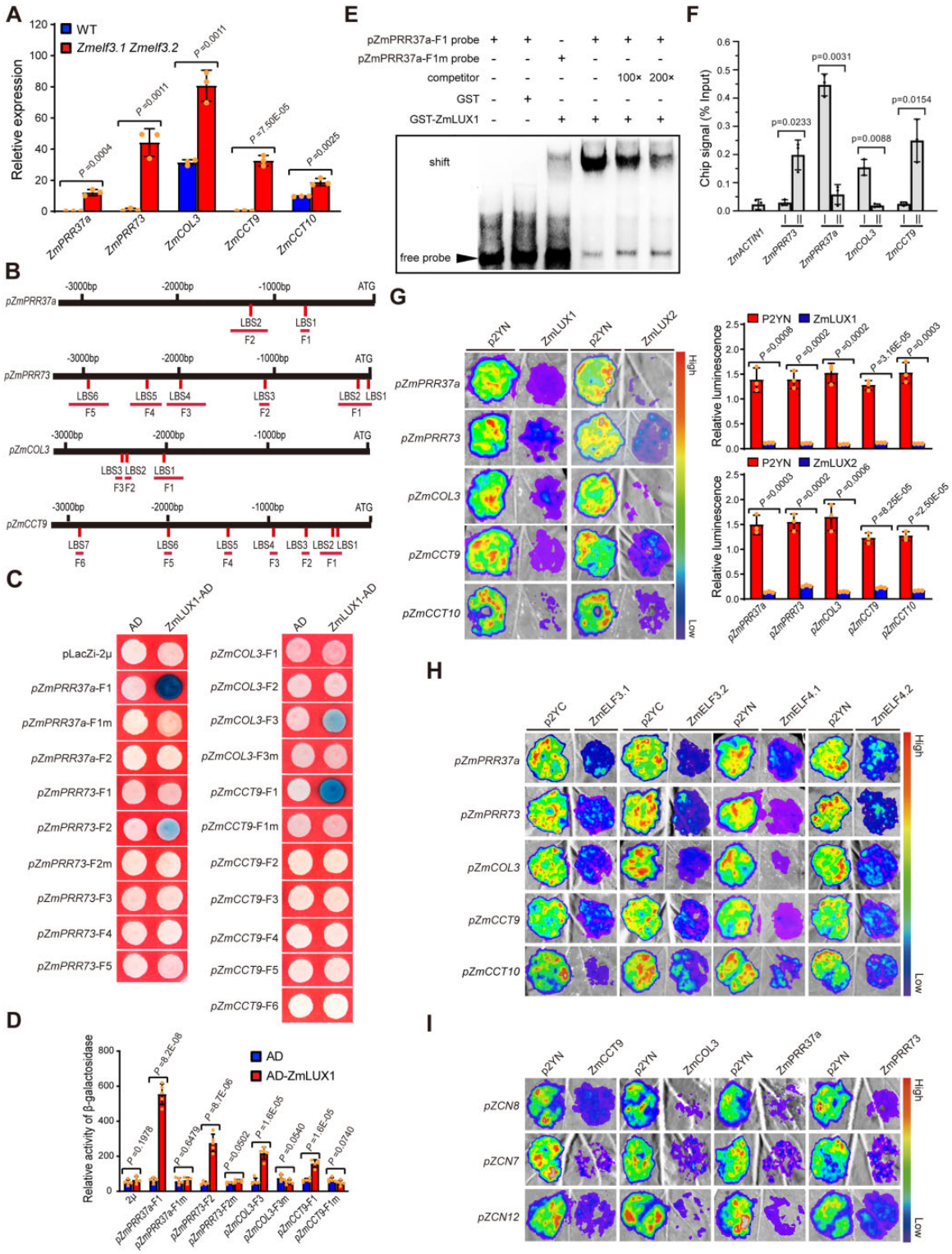

Figure 4 Maize EC directly represses the expression of several flowering repressor genes. A, RT-qPCR assay showing that the expression levels of several flowering repressor genes, *ZmPRR37a*, *ZmPRR73*, *ZmCOL3*, *ZmCCT9*, and *ZmCCT10*, are significantly upregulated in the *Zmelf3.1 Zmelf3.2* double mutant compared to the WT (ZC01). Values are means ± SD (n = 3 technical replicates). Two biological replicates were performed and the results were similar (leaves from six plants were used for each biological replicate). B, The promoters of the above flowering repressor genes harbor multiple typical LUX binding sites (LBS, 5′-GATWCG-3′, 5′-GATWKG-3′, or 5′-GATWCY-3′, where W indicates A or T, K indicates C or T, and Y indicates G or T). The positions of the LBS motifs in each promoter are indicated with red vertical lines and the promoter fragments used for Y1H assay are marked with red horizontal lines. C, Y1H assay showing that ZmLUX1 directly binds to specific promoter fragments containing the LBS motif of *ZmPRR37a* (5′-CGTATCGTATC-3′), *ZmPRR73* (5′-GATTCG-3′), *ZmCOL3* (5′-GATTCG-3′), and *ZmCCT9* (5′-AGAATC CATATC-3′). For mutagenesis, the LBS motif was mutated to 5′-TCCAAGTGATG-3′ in *ZmPRR37apro*-F1, 5′-CACACA-3′ in *ZmPRR73pro*-F2, 5′-CTAGGA-3′

(continued)

flowering (Nakamichi et al., 2005). We showed here that in maize, the EC directly represses the expression of the flowering repressor genes *ZmCCT9*, *ZmCCT10*, *ZmCOL3*, *ZmPRR37a*, and *ZmPRR73*, thereby alleviating the suppression of the expression of *ZCN8*, *ZCN7*, and *ZCN12* mediated by their encoding proteins, to promote flowering under both SD and LD conditions (Figure 7). Thus, it appears that the switch in EC function (promoting flowering in SD plants and repressing flowering in LD plants) resides in the downstream signaling pathway in SD and LD plants.

The circadian clock is also implicated in temperature regulation of flowering time through temperature entrainment, which allows plants to perceive and respond to temperature cues, and adjust clock gene expression accordingly. In addition, the circadian clock can help maintain clock gene expression over a wide range of temperature through a mechanism termed temperature compensation (Salome et al., 2010). It is notable that recent studies have shown that the polyQ repeats and PrD of Arabidopsis ELF3 play a role in mediating thermal responsiveness (Undurraga et al., 2012; Jung et al., 2020). In addition, Arabidopsis ELF3 was shown to physically interact with and suppress the transcriptional activation activity of PIF4 in an EC-independent manner to regulate hypocotyl growth (Nieto et al., 2015). Moreover, ELF3 was recently shown to directly regulate the expression of *PIF4* in thermoresponsive growth (Raschke et al., 2015), while ELF3 regulates circadian gating of the shade avoidance response in Arabidopsis through physically interacting with and repressing the DNA-binding activity of PIF7, thus antagonizing PIF7-induced gene expression and hypocotyl growth (Jiang et al., 2019). Intriguingly, we found that ZmELF3s in all the analyzed tropical and temperate maize lines lack the polyQ repeats and a typical PrD (Supplemental Data Set S7), hinting that ZmELF3s might not be involved temperature responsiveness. However, a recent study reported that the expression of a number of core clock genes (*CCA1*, *GIGANTEA*, *PRR59*, *PRR73*, *PRR95*, and *LUX*) in barley responds rapidly to changes in temperature and that this response is lost in *elf3* mutants, indicating that the temperature response in dependent on a functional ELF3 protein (which also lacks the polyQ repeats and typical PrD domain) in barley (Ford et al., 2016). Thus, it will be an interesting research avenue to further clarify whether ZmELF3s play a role in temperature regulation of flowering time and shade avoidance response in future studies.

Previous studies have suggested that the spread of maize from tropical to temperate regions entailed stepwise regulatory changes in multiple flowering time genes. Available data suggest that SNP-1245 in the promoter of *ZCN8*, which is associated with differential binding of the flowering activator ZmMADS1, was first selected and nearly fixed in early domestication of maize. Then, another variant in the *ZCN8* promoter, InDel-2339, which most likely originated from *Z. mays ssp. Mexicana*, was introgressed into maize and further selected during the spread of maize from tropical to temperate regions (Guo et al., 2018). Similarly, insertion of a MITE upstream of the *vgt1* region, the CATCA-like transposable element upstream of *ZmCCT10* and the *Harbinger*-like transposable element upstream of *ZmCCT9* likely occurred after the initial domestication of maize, as they are not observed in surveyed teosinte accessions and the frequencies of their early flowering alleles rose when maize spread into the Northern USA (but not South America) (Yang et al., 2013; Huang et al., 2018). In this study, we discovered that two closely linked retrotransposons located in the *ZmELF3.1* promoter upregulate *ZmELF3.1* expression, and that they were already present in some accessions of teosinte, thus representing preexisting standing variations that were selected postdomestication for adaptation to temperate regions during the pre-Columbian era, both Northward and Southward (Figure 6, B–D). Analogous to our finding, a recent study reported that ancestral Puebloan people selected temperate-adapted maize for 2,000 years in situ in the southwestern USA and the early flowering alleles were from preexisting standing variation in teosinte (Swarts et al., 2017). In addition, the increased frequency of the retrotransposon-harboring haplotype in modern temperate inbred lines suggests that *ZmELF3.1* is still under selection during modern temperate maize breeding (Figure 6A). Moreover, the finding that the LTR/*Gypsy* retrotransposon

Figure 4 (Continued)
in *ZmCOL3pro*-F3, and 5′-CTAGGA TCCTAG-3′ in *ZmCCT9pro*-F1. Three independent experiments showed similar results. D, Quantification of ZmLUX1 binding activity. Five independent yeast clones were used for activity determination. Values are means ± SD (n = 5 independent clones). Significant differences were determined by the Student's t test. E, EMSA showing that recombinant GST-ZmLUX1 fusion protein binds to a biotin-labeled probe of the *ZmPRR37a* promoter. GST protein was used as a negative control. Two independent experiments were performed, with similar results. F, ChIP-qPCR assay of enrichment for ZmELF3.1 at the *ZmPRR37a*, *ZmPRR73*, *ZmCOL3*, and *ZmCCT9* promoters in the leaves of V2-stage *Ubipro:ZmELF3.1-EGFP* transgenic seedlings grown under LD conditions. The "I" and "II" represent the individual amplified fragment of each promoter as shown in (B). Values are means ± SD (n = 3 biological replicates, leaves from six plants were used for each replicate). P-value was determined by the Student's t test. Two independent experiments showed similar results. G, Transient expression assay showing that ZmLUX1 and ZmLUX2 repress the expression of the above flowering repressor genes. Values are means ± SD (n = 3 different infiltrated regions). At least six independent experiments were performed, with similar results. Representative images of *N. benthamiana* leaves 72 h after infiltration are shown. Significant differences were determined by the Student's t test. H, Transient expression assay shows that both *ZmELF3s* and *ZmELF4s* suppress the expression of *ZmPRR37a*, *ZmPRR73*, *ZmCOL3*, and *ZmCCT9*. At least six independent experiments were performed, with similar results. Representative images of *N. benthamiana* leaves 72 h after infiltration are shown. I, Transient expression assay shows that *ZmPRR37a*, *ZmPRR73*, *ZmCOL3*, and *ZmCCT9* suppress the expression of *ZCN8*, *ZCN7*, and *ZCN12*. At least six independent experiments were performed, with similar results. Representative images of *N. benthamiana* leaves 72 h after infiltration are shown.

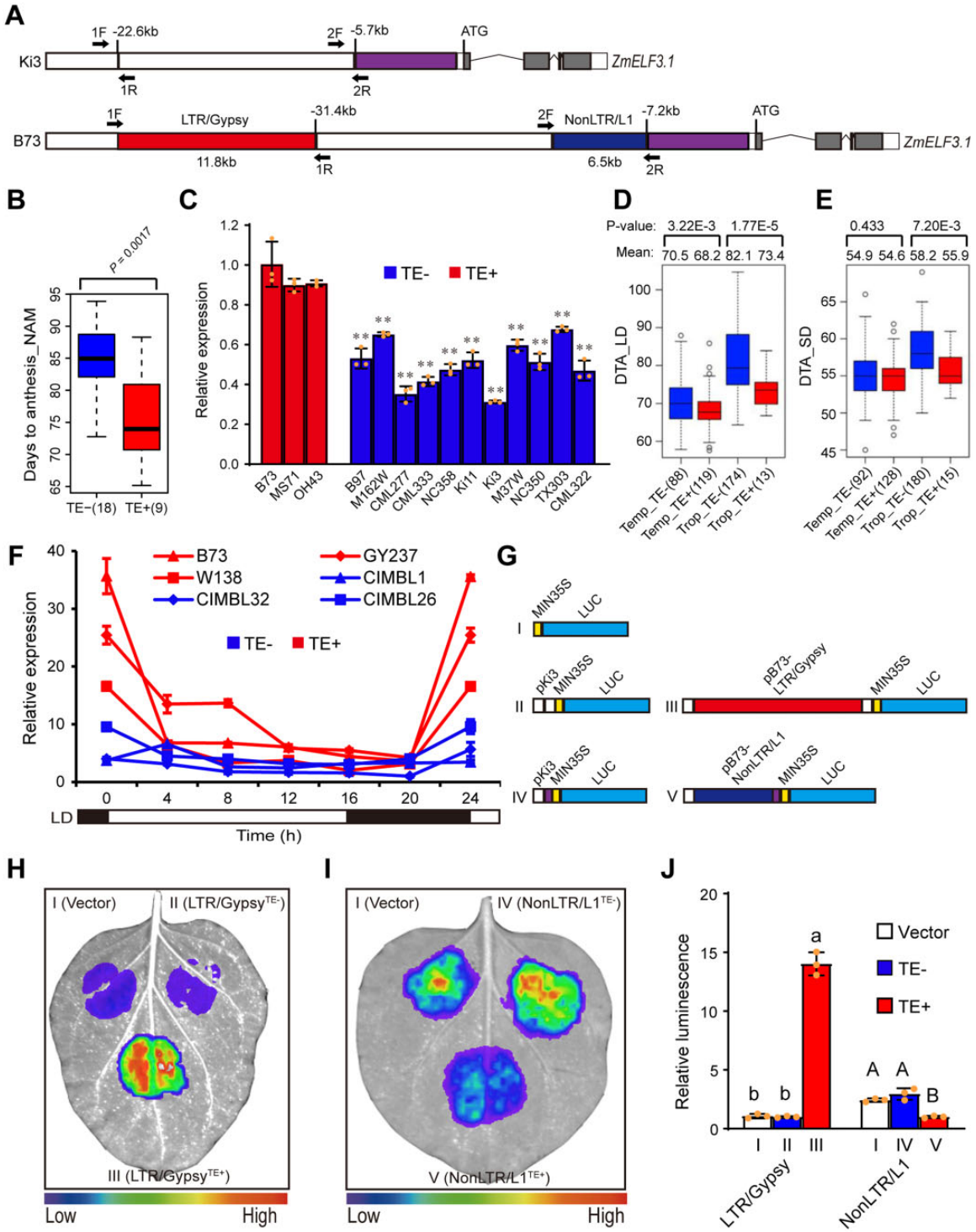

Figure 5 The NonLTR/L1 retrotransposon and LTR/*Gypsy* retrotransposon regulate *ZmELF3.1* expression. A, Schematic diagram of the locations of a NonLTR/*L1*-type retrotransposon (6.5 kb in length) and an LTR/*Gypsy* type retrotransposon (11.8 kb in length) in two representative inbred lines (B73 and Ki3). 1F/1R and 2F/2R indicate the primers used to construct the vectors in Figure 5G. B, Flowering time of the NAM founder lines with or without the retrotransposons. The flowering time data were obtained from the previous NAM flowering-time mapping study (Buckler et al., 2009). C, The relative expression levels of *ZmELF3.1* in the NAM founder lines with retrotransposon insertion upstream of *ZmELF3.1* promoter are significantly higher than in the NAM founder lines without retrotransposon insertion. Values are means ± SD (n = 3 biological replicates, leaves from six plants were used for each replicate). D and E, Flowering time of 415 maize inbred lines (Yang et al., 2014) with or without retrotransposons in the *ZmELF3.1* promoter under LD (D) or SD (E) conditions. The number of inbred lines is indicated in brackets. F, The relative expression levels of *ZmELF3.1* in inbred lines with retrotransposon insertion upstream of *ZmELF3.1* promoter are significantly higher than in the inbred lines without retrotransposon insertion. Three independent experiments were performed, with similar results. G, Schematic diagrams of the constructs used to test the effect of the two retrotransposon elements on gene expression in transient expression assay in *N. benthamiana* leaves.

(continued)

strongly activates, while the NonLTR/*L1* retrotransposon mildly represses the expression of *ZmELF3.1* (Figure 5, G and J) suggests a possibility of breaking their linkage or deleting the inhibitory retrotransposon using genome editing to create novel alleles of *ZmELF3.1* for earlier flowering and adapting to even higher altitudes. Thus, the identification of more flowering genes and their allelic variation via tapping into the vast diversity of maize germplasm offers the promise to breed maize cultivars that adapt more efficiently to the next century of changing environments through harnessing standing natural variation or creating new variants via genome editing.

Methods

Plant materials and growth conditions

All maize (*Z. mays*) lines used in this study were in the B73 or ZC01 inbred line backgrounds, unless other specified. For gene cloning, the seeds of B73 were directly sown on soil (Pindstrup Substrate No 2, Pindstrup Mosebrug A/S, Ryomgaard Denmark) and grown in a growth chamber under LD conditions (28°C 16-h light/22°C 8-h dark). For analysis of gene expression, maize seeds were directly sown on soil and grown in a growth chamber under either LD (16-h light/8-h dark) or SD (8-h light/16-h dark) conditions with 300 μmol m^{-2} s^{-1} light intensity provided by full-spectrum white fluorescent light tubes. The humidity was set to 60%, and the daytime and nighttime temperature was set to 28°C and 22°C, respectively. For phenotypic analysis, seeds of the mutant and WT control (ZC01) were sown in the field either under natural LD (Langfang, Hebei Province, China; 39.53°N, 116.72°E, 15-h light/9-h dark) or natural SD (Sanya, Hainan Province, China; 18.73°N, 109.17°E, 11-h light/13-h dark) conditions.

The WT and *elf3-7* mutant of Arabidopsis (*A. thaliana*) used in this study were in the Columbia-0 accession (Reed et al., 2000). All Arabidopsis transgenic plants used in this study were generated in the *elf3-7* background. Arabidopsis seeds were surface-sterilized with 5% [v/v] NaClO solution for 15 min and washed with sterile water for 3 times, then plated on half-strength Murashige and Skoog solid medium (1% [w/v] sucrose and 0.8% [w/v] agar, pH 5.8) and incubated in the dark at 4°C for 3 d for stratification. Thereafter, they were moved to the culture room under white light with 200 μmol m^{-2} s^{-1} light intensity provided by full-spectrum white fluorescent light tubes at 23°C (16-h light/8-h dark) for 10 d, then transplanted to soil.

Nicotiana benthamiana seeds were directly sown on soil and grown in the same culture room as Arabidopsis for about 1 month before use.

GWAS

A NAM population comprising 5,000 RILs was developed from crosses between B73 as a common parent and 25 other various inbred lines (Buckler et al., 2009). This NAM population was evaluated across 13 environments, consisting of eight environments in the USA (Buckler et al., 2009) and five environments in China (Li et al., 2016). The best linear unbiased predictions for flowering time for all NAM RILs, derived across these 13 environments, were calculated using a mixed model in SAS (Version 9.2, SAS Institute; Flint et al., 2011). The SNP markers around the target gene for the NAM population (http://panzea.org.com/) were selected for inclusion in the regional association mapping. The association analysis was conducted using TASSEL version 5.0 software (Bradbury et al., 2007), in which the mixed linear model with population structure (3 PCAs) and pair-kinship (K matrix) treated as covariates was applied to test for association between segregating sites and phenotypes (Yu et al., 2005). Linkage disequilibrium analysis within the target region was conducted using Haploview software (Barrett et al., 2004).

Phylogenetic and conserved motifs analysis

The homologous protein sequences for ELF3, ELF4, and LUX were retrieved from TAIR (https://www.arabidopsis.org/, for Arabidopsis), or gramene (http://ensembl.gramene.org/genome_browser/index.html, for maize and rice). The full-length amino acid sequences were aligned using the MUSCLE multiple sequence alignment program (Edgar, 2004), and the phylogenetic trees were constructed using the neighbor-joining method of MEGA version 7. The bootstrap method was used for statistical support for nodes in the phylogenetic tree. The number of bootstrap replications was 500. The Poisson model was used for substitutions model analysis to obtain tree branch lengths (Kumar et al., 2016). The alignments for the phylogenetic analysis are provided as Supplemental Files S1–S6. Conserved motifs were identified using MEME software (Bailey et al., 2006).

RNA extraction and RT-qPCR analysis

Various plant samples were collected and immediately frozen in liquid nitrogen and stored at −80°C. Total RNA was extracted using Trizol reagent (Invitrogen, Waltham, MA, USA) from three independent pools of tissues, and first-strand cDNAs were synthesized using a reverse transcription kit (TIANGEN, Beijing, China) according to the manufacturer's instructions. The cDNA was diluted 1:5 and RT-qPCR was performed using SuperReal PreMix Plus (TIANGEN) with a 7500 real-time PCR detection system (Applied Biosystems, Waltham, MA, USA). *ZmTubulin5* and *AtACT2*

Figure 5 (Continued)
H and I, The LTR/*Gypsy* retrotransposon strongly activates *ZmELF3.1* expression while the NonLTR/*L1* retrotransposon mildly inhibits *ZmELF3.1* expression. Representative images of *N. benthamiana* leaves 72 h after infiltration are shown. Three independent experiments were performed, with similar results. J, Quantification of luminescence intensity in (H) and (I). Values are means ± SD (n = 3 biological replicates). Significant differences was determined by Duncan's multiple-range test in Fig. 5J and Student's t test in the others. Three independent experiments were performed, with similar results.

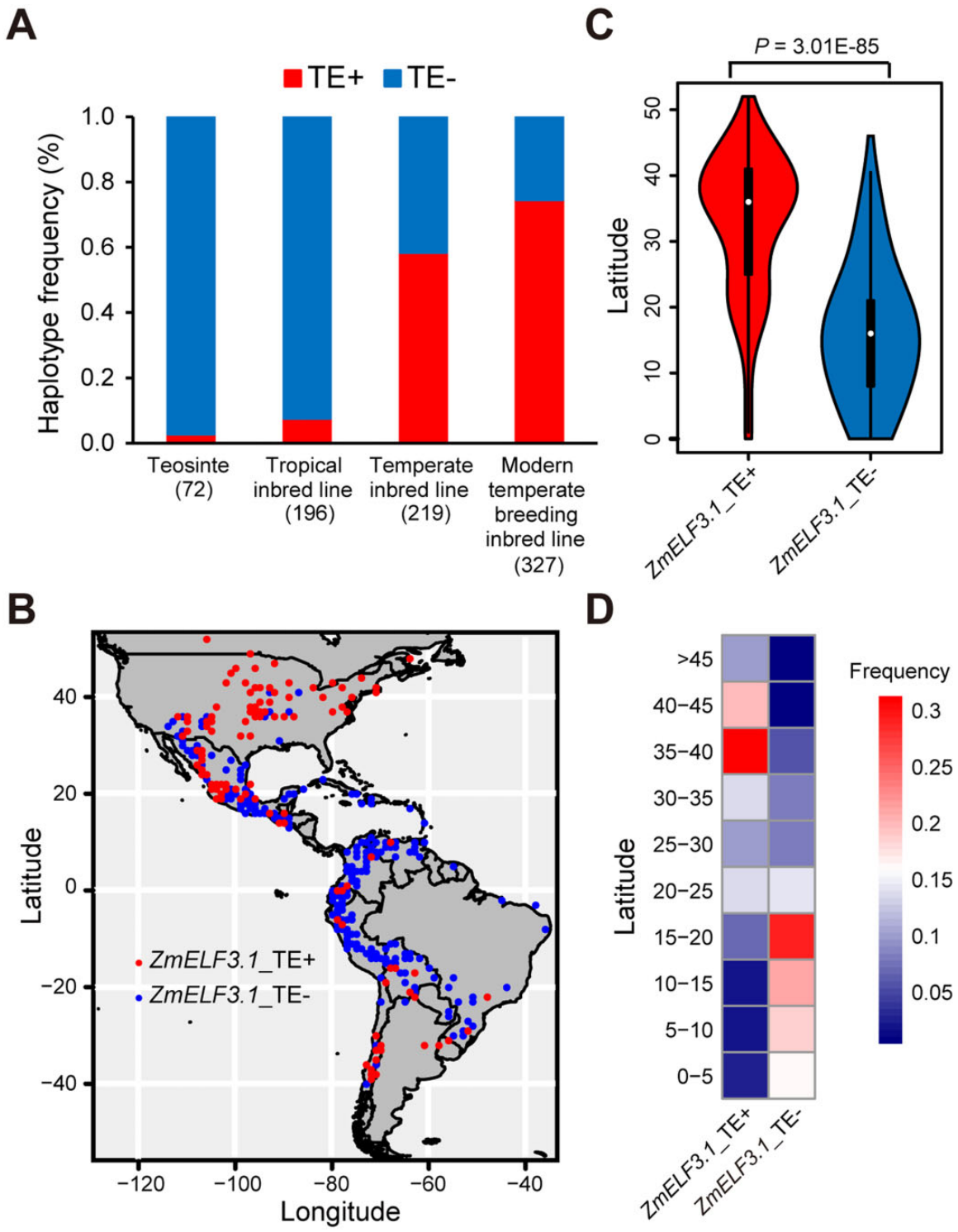

Figure 6 *ZmELF3.1* was selected during the spread of maize from tropical to temperate regions. A, Frequency of the retrotransposons in the *ZmELF3.1* promoter across teosinte, tropical maize, temperate inbred lines, and modern temperate breeding inbred lines. The number of various germplasms is indicated in parentheses. B, Geographic distribution of 1,008 maize landraces native to the Americas with or without the retrotransposon insertions in the *ZmELF3.1* promoter (Huang et al., 2018). C, Accessions with retrotransposons insertion at *ZmELF3.1* predominantly accumulate at higher latitudes, whereas accessions without the retrotransposon insertions at *ZmELF3.1* mainly distribute at low latitudes. Significant differences were determined by the Student's *t* test. D, Frequency of accessions with or without the retrotransposon insertions at *ZmELF3.1* along a latitudinal gradient.

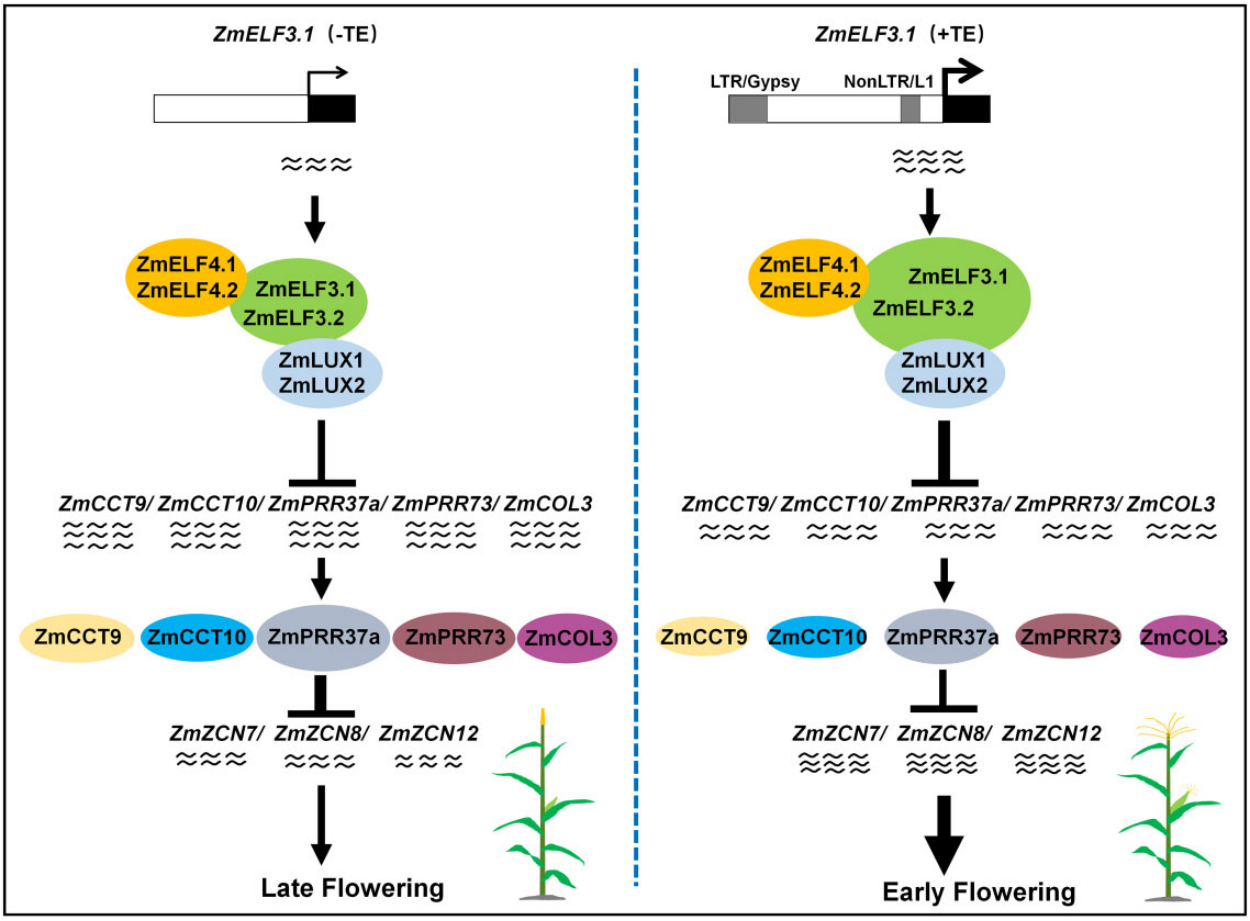

Figure 7 Schematic model illustrating a role of the EC in regulating flowering time in maize. ZmELF3.1/3.2 bridge ZmELF4.1/4.2 and ZmLUX1/2 to form ECs, and then the EC directly represses the expression of a set of flowering repressor genes: *ZmCCT9*, *ZmCCT10*, *ZmCOL3*, *ZmPRR37a*, and *ZmPRR73*, thereby relieving their suppression on expression of three maize florigen genes (*ZCN8*, *ZCN7*, and *ZCN12*), to promote flowering. Insertion of an LTR/*Gypsy* and a NonLTR/*L1* retrotransposon upstream of *ZmELF3.1* enhances the expression of *ZmELF3.1*, thus promoting flowering. Arrow: activation; Bar: repression.

were used as the internal controls for maize and Arabidopsis genes, respectively. The $2^{-\triangle\triangle CT}$ method was used to determine the relative expression levels of target genes (Schmittgen and Livak, 2008).

Protein subcellular localization assay

The coding sequences without stop codon of *ZmELF3*s, *ZmELF4*s, and *ZmLUX*s were obtained by PCR using maize B73 cDNA as template, and cloned into the pCAMBIA1305-EGFP binary vector digested with *Xba*I to generate the *E35Spro:ZmELF3s-EGFP-TNos*, *E35Spro::ZmELF4s-EGFP-TNos*, and *E35Spro:ZmLUXs-EGFP-TNos* constructs, respectively (primers are listed in Supplemental Data Set S8). The constructs were then introduced into Agrobacterium (*Agrobacterium tumefaciens*) strain EHA105 by electroporation (BIORAD, Hercules, CA, USA). To determine the subcellular localization of ZmELF3s, ZmELF4s, and ZmLUXs proteins, Agrobacterium EHA105 colonies individually carrying each of the above constructs or the nuclear marker *E35Spro:AHL22-ERFP-TNos* (Xiao et al., 2009) were harvested by quick centrifugation and resuspended to a cell density (OD_{600}) of 1.0 in infiltration solution (10 mM $MgCl_2$, 10 mM MES pH 5.7, and 150 μM acetosyringone; Wydro et al., 2006), and then co-infiltrated into *N. benthamiana* leaves in an equal volume. Two days after infiltration, GFP and RFP signals were observed under a confocal microscope using a 488-nm laser for excitation and an emission wavelength of 526 nm with 30% power (Zeiss LSM710).

Creation of transgenic lines in Arabidopsis and maize

PCR-amplified coding sequences without stop codon of the *ZmELF3* genes were cloned into the CPB-Ubi-EGFP binary vector digested with *Pst*I and *Bam*HI to be placed under the control of the maize *Ubiquitin* promoter and the *TNos* terminator to obtain the *Ubipro:ZmELF3s-EGFP-TNos* expression cassettes (primers are listed in Supplemental Data Set S8). The constructs were then introduced into Agrobacterium strain GV3101 and separately transformed into the Arabidopsis *elf3-7* mutant using the floral dip method (Clough and Bent, 1998) to obtain *elf3-7 ZmELF3*-OE lines. More than 10 independent transgenic lines for each

transformation were obtained by selection on glufosinate ammonium and two independent lines were selected for further studies.

The above *Ubipro::ZmELF3s-EGFP* constructs were also introduced into Agrobacterium strain EHA105 and transformed into the maize inbred line ZC01 using immature embryos (Ishida et al., 2007). Two and three independent transgenic lines were obtained for *ZmELF3.1* and *ZmELF3.2*, respectively.

Generation of the CRISPR/Cas9 *ko* lines in maize

To obtain the *ko* mutants of *ZmELF3.1/3.2* and *ZmLUX1/2*, a CRISPR/Cas9 *ko* vector was constructed according to our previously described method with minor modifications: the *E35S* promoter and the *AtU6-26* promoter were replaced with the maize *Ubiquitin* promoter and the *ZmU6-6* promoter, respectively (Zhao et al., 2016). Multiple target sites were identified with SnapGene Viewer version 2.4.3 software based on the criteria of 5′ G-$(N)_{19}$-NGG 3′. All putative target sequences were then checked against the B73 genomic sequence at the gramene database by BLAST for specificity. Specific target sequences without PAM together with the universal scaffold sequence were used for prediction of the single-guide RNA (sgRNA) secondary structure with the program RNA Folding Form (http://unafold.rna.albany.edu/?q=mfold/RNA-Folding-Form2.3; Zuker, 2003) to select those target sites that did not affect the secondary structure of the universal scaffold sequence. Since the target sites were designed based on the B73 genome, and the inbred line ZC01 was used for transformation, we designed a pair of primers to amplify fragments containing the target sites and sequenced the PCR products amplified from ZC01 (primers are shown in Supplemental Data Set S8). Sequence alignment showed that target 1 of *ZmELF3.1* has one base mismatch between B73 and ZC01, while the other three targets had identical sequences between B73 and ZC01 (Supplemental Data Set S1). The four target sequences of ZC01 were separately introduced into four sgRNA expression cassettes (pZmU6-6 + target + universal scaffold sequence) by overlapping PCR (Urban et al., 1997). The four sgRNA expression cassettes were then sequentially cloned into the pCPB-ZmUbi::hSpCas9 vector (Zhao et al., 2016) using the *Hin*dIII restriction site. Each clone was verified by PCR and sequencing. The resulting final vector was introduced into Agrobacterium strain EHA105 and transformed into the maize inbred line ZC01 using immature embryo. Eighteen independent transgenic lines were obtained. Through sequencing analysis, we selected three independent lines for *Zmelf3.1* single mutants (ko#1, ko#2, and ko#3), three independent lines of *Zmelf3.2* single mutants (ko#4, ko#5, and ko#6), and three independent lines of *Zmelf3.1 Zmelf3.2* double mutants (ko#7, ko#8, and ko#9) for self-pollination to obtain various homozygous mutants. For *ZmLUX1/2*, two independent transgenic lines each for *Zmlux1*, *Zmlux2*, and *Zmlux1 Zmlux2*, were selected for further study. The produced T_2 generation progenies together with the WT (ZC01) were planted under natural LD and SD conditions for observation of flowering time and other phenotypes.

Y1H assay

The Y1H was performed using the pJG4-5 vector (Clontech, Mountain View, CA, USA) encoding the GAL4 activation domain and pLacZi-2μ vector harboring the bacterial *lacZ* reporter gene as described previously (Lin et al., 2007). The full-length coding region of *ZmLUX1* was cloned into the pJG4-5 vector digested with *Xho*I to generate *AD-ZmLUX1*. To obtain the *ZmCCT9pro::LacZ*, *ZmCOL3pro::LacZ*, *ZmPRR37apro::LacZ*, and *ZmPRR73pro::LacZ* reporter constructs, the promoter fragments of *ZmCCT9*, *ZmCOL3*, *ZmPRR37a*, and *ZmPRR73* were individually PCR amplified from B73 genomic DNA and then inserted into the pLacZi-2μ vector digested with *Eco*RI and *Xho*I (primers are listed in Supplemental Data Set S8). For mutagenesis of the LBS motif in the promoter fragments above, primer pairs were designed according to Agilent Technologies (http://www.genomics.agilent.com) and used to generate plasmids containing mutated LBS motif following the manufacturer's instructions. The indicated plasmid pairs were then co-transformed into the yeast strain EGY48 with PEG3350-LiAc-mediated transformation. The positive transformants screened on synthetic defined medium lacking Trp and Ura (SD−Trp −Ura, Clontech) were transferred to chromogenic medium containing raffinose, galactose, and 5-bromo-4-chloro-3-indolyl-beta-d-galactopyranoside (Amresco) for blue color development. To quantify β-galactosidase activity, the positive clones were grown in liquid SD −Trp −Ura medium overnight, harvested by centrifugation and resuspended in Z-buffer (40 mM NaH_2PO_4, 60 mM Na_2HPO_4, 1 mM $MgSO_4$, 10 mM KCl, pH 7.0, 50 mM β-mercaptoethanol) and then lysed with chloroform and 0.1% (w/v) sodium dodecyl sulfate. The substrate ONPG was added to the supernatants and incubated at 30°C for 5 min and then 1 M Na_2CO_3 was immediately added to terminate the reaction. After a brief centrifugation to settle cell debris, the values of OD_{420} and OD_{600} were measured from the supernatants and the original liquid cultures, respectively.

Y2H assay

The complete coding sequences of *ZmELF3.1*, *ZmELF3.2*, *ZmELF4.1*, *ZmELF4.2*, *ZmLUX1*, and *ZmLUX2* were obtained by PCR from a cDNA library prepared from 2-week-old B73 seedlings (primers are listed in Supplemental Data Set S8). The cDNAs of *ZmELF3.1*, *ZmELF3.2*, *ZmELF4.1*, and *ZmELF4.2* were then cloned into the pGADT7 vector (Clontech) to produce the AD-ZmELF3 and AD-ZmELF4 fusion proteins, while the cDNAs of *ZmELF4.1*, *ZmELF4.2*, *ZmLUX1*, and *ZmLUX2* were cloned into the pGBKT7 vector (Clontech) to produce the *BD-ZmELF4* and *BD-ZmLUX*s fusion proteins. The plasmid combinations between *AD*, *AD-ZmELF3*, *AD-ZmELF4*, and *BD*, *BD-ZmLUX*s, and *BD-ZmELF4* were co-transformed into the yeast strain AH109 following the manufacturer's instructions (Clontech). Positive yeast clones were screened on SD −Leu −Trp medium and then spotted

onto plates containing SD −Leu −Trp and SD −Leu −Trp −His with 5 mM 3-amino-1,2,4-triazole (3-AT) for growth.

Yeast three-hybrid assay

For yeast three-hybrid assay, full-length coding sequences (cDNAs) of *ZmLUX1* and *ZmLUX2* were cloned into the pBridge vector (Clontech) at the *Eco*RI site to generate *BD-ZmLUX1* and *BD-ZmLUX2*, respectively. The cDNAs of *ZmELF3.1* and *ZmELF3.2* were then further ligated into the generated constructs above at the *Bgl*II site to produce the *BD-ZmLUX-ZmELF3* constructs (primers are listed in Supplemental Data Set S8). The combinations between AD- and BD-fused plasmids were co-transformed into yeast strain AH109 and the positive yeast colonies were screened on selective medium (SD −Leu/−Trp). The positive clones were spotted onto plates of SD −Leu −Trp or SD −Leu −Trp−His-Met with 1 mM 3-AT for growth.

Recombinant protein production

For protein production and purification, the coding sequence of *ZmLUX1* was amplified from the above *BD-ZmLUX1* plasmid and cloned into the pGEX-4T-1 vector at the *Eco*RI restriction site to generate the *GST-ZmLUX1* construct, which was transformed into *Escherichia coli* strain Transette (TransGen Biotech, China). The production of GST-ZmLUX1 recombinant protein was induced by the addition of 0.4 mM isopropyl β-D-thiogalactopyranoside and growth at 16°C overnight before purification with glutathione sepharose resin (GE Healthcare, Chicago, IL, USA) according to the manufacturer's protocol.

Gel mobility shift assay

The direct binding of ZmLUX1 to the *ZmPRR37a* promoter was assessed using an EMSA kit (Beyotime, Jiangsu, China) following the manufacturer's protocol with probes listed in Supplemental Data Set S8. The GST (glutathione S-transferase) proteins were used as the controls.

ChIP-qPCR assay

The leaves from V2-stage *UBIpro::ZmELF3.1-EGFP* transgenic seedlings grown under LD conditions were crosslinked with 1% (w/v) formaldehyde and ground in liquid nitrogen. The chromatin complex was prepared following the method of Xie et al. (2020). In brief, the supernatant was precleared with 40 µL Protein-A-Agarose (16-157, EMD Millipore Corp., Burlington, MA, USA) and incubated at 4°C for 1 h. The supernatant was then incubated with 50 µL anti-GFP Magarose beads (SM038001, SMART Lifesciences) at 4°C overnight. After washing, the immune complex was eluted from the beads with elution buffer (1% SDS and 0.1 M $NaHCO_3$) and harvested the supernatant (eluate) by centrifugation. The precipitated DNA was then recovered and quantified using quantitative PCR with the primer pairs listed in Supplemental Data Set S8. The values were normalized to input DNA to obtain the fold-enrichment. *ACTIN1* was used as the internal control.

BiFC assay

The cDNAs of *ZmELF3.1* and *ZmELF3.2* were individually cloned into the p2YC vector (digested with *Pac*I and *Spe*I) encoding C-terminal YFP fragments to generate the *ZmELF3.1-cYFP* and *ZmELF3.2-cYFP* constructs. The cDNAs of *ZmELF4.1*, *ZmELF4.2*, *ZmLUX1*, and *ZmLUX2* were separately cloned into the similarly *Pac*I-*Spe*I digested p2YN vector (Walter et al., 2004; Yang et al., 2007) encoding N-terminal YFP fragments to obtain *ZmELF4.1-nYFP*, *ZmELF4.2-nYFP*, *ZmLUX1-nYFP*, and *ZmLUX2-nYFP*, respectively (primers are listed in Supplemental Data Set S8). Various combinations of these constructs were introduced into Agrobacterium strain EHA105 and co-infiltrated into *N. benthamiana* leaves with the viral silencing suppressor P19 and the nuclear protein marker *AHL22-ERFP*. The infiltrated *N. benthamiana* plants were grown in the dark for 48 h, then grown in the light for 3–6 h before observation with a confocal microscope (Zeiss LSM710).

LCI assay

The vectors pCAMBIA1300-nLUC and pCAMBIA1300-cLUC were used for LCI assay according to previously described procedures (Chen et al., 2008). The coding sequences of *ZmELF3.1* and *ZmELF3.2* were ligated into the pCAMBIA1300-nLUC vector at the *Kpn*I-*Sal*I sites to generate the *ZmELF3.1-nLUC* and *ZmELF3.2-nLUC* vectors, respectively. The coding sequences of *ZmELF4.1*, *ZmELF4.2*, *ZmLUX1*, and *ZmLUX2*, were ligated into the pCAMBIA1300-cLUC vector at the *Kpn*I-*Sal*I sites to produce the *ZmELF4.1-cLUC*, *ZmELF4.2-cLUC*, *ZmLUX1-cLUC*, and *ZmLUX2-cLUC* vectors, respectively (primers are listed in Supplemental Data Set S8). The constructs were individually transformed into Agrobacterium strain EHA105 and co-infiltrated into *N. benthamiana* leaves using the indicated plasmid combinations and Agrobacterium strain EHA105 carrying the P19 vector was simultaneously infiltrated with each combination. The infiltrated plants were first grown under dark for 24 h and then in the light (16-h light/8-h dark) for 24–48 h. Luciferase activity was acquired with the Plant Imaging System of NightShade LB985 (Berthold Technologies, Bad Wildbad, Germany) after applying 20 mg/mL D-luciferin potassium salt (Gold Biotech, St. Louis, MO, USA).

Transient expression assay

Transient expression assays were carried out with the vector pGreenII 0800-LUC (Dual-LUC) as described previously (Hellens et al., 2005). To obtain the *ZmCCT9pro::LUC*, *ZmCCT10pro::LUC*, *ZmCOL3pro::LUC*, *ZmPRR37apro::LUC*, *ZmPRR73pro::LUC*, *ZCN8pro::LUC*, *ZCN7pro::LUC*, and *ZCN12pro::LUC* reporter constructs, the promoters (~3 kb) of *ZmCCT9*, *ZmCCT10*, *ZmCOL3*, *ZmPRR37a*, *ZmPRR73*, *ZCN8*, *ZCN7*, and *ZCN12* were amplified from B73 genomic DNA and ligated into the vector pGreenII 0800-LUC at the *Hin*dIII site (primers are listed in Supplemental Data Set S8). Agrobacterium colonies (strain EHA105) carrying the

indicated plasmid combinations were co-infiltrated into *N. benthamiana* leaves together with Agrobacterium strain EHA105 harboring P19. Subsequent processing was the same as the LCI assay.

Statistical analysis

To assess statistical significance of the experimental data, Student's *t* tests were employed to determine significant differences between two groups. If more than two groups of data are analyzed, one-way analysis of variance was adopted using the commercially available package SAS (version 9.2, SAS Institute, Cary, NC, USA) and Duncan's multiple-range test was used for all pairwise comparisons with *P*-values corrected for multiple comparisons to control against type I errors (Brady et al., 2015).

Accession numbers

The genes studies in this article are under the following accession numbers: *AtELF3* (At2g25930), *AtACT2* (At3g18780), *ZmELF3.1* (Zm00001d044232), *ZmELF3.2* (Zm00001d039156), *ZmTubulin5* (Zm00001d006651), *ZmELF4.1* (Zm00001d047269), *ZmELF4.2* (Zm00001d020364), *ZmLUX1* (Zm00001d011785), *ZmLUX2* (Zm00001d041960), *ZmLUX3* (Zm00001d010280), *ZmLUX4* (Zm00001d038191), *ZmCCT9* (Zm00001d000176), *ZmCCT10* (Zm00001d024909), *ZmCOL3* (Zm00001d017176), *ZmPRR37a* (Zm00001d022590), *ZmPRR73* (Zm00001d047761), *ZCN7* (Zm00001d038725), *ZCN8* (Zm00001d010752), *ZCN12* (Zm00001d043461), *OsELF3.1* (Os06g0142600), *OsELF3.2* (Os01g0566050), *OsELF4.1* (Os06g0142600), *OsELF4.2* (Os01g0566050), *OsELF4.3* (Os06g0142600), *OsLUX1* (Os01g0971800), *OsLUX2* (Os05g0412000) and *OsLUX3* (Os01g0844900).

Supplemental data

The following materials are available in the online version of this article.

Supplemental Figure S1. Amino acid sequence comparison and phylogeny of ZmELF3.1/3.2 with AtELF3 and OsELF3.1/3.2.

Supplemental Figure S2. Amino acid sequence comparison and phylogeny of ELF4 and LUX orthologs from Arabidopsis, maize, and rice.

Supplemental Figure S3. Both *ZmELF3.1* and *ZmELF3.2* rescue the Arabidopsis *elf3-7* mutant phenotypes when overexpressed.

Supplemental Figure S4. Loss-of-function of *ZmELF3.1* results in greater plant height and ear height.

Supplemental Figure S5. Generation of *Zmlux ko* mutants using CRISPR/Cas9.

Supplemental Figure S6. WT plants and *ZmELF3.1* overexpressors show no significant differences in flowering time.

Supplemental Figure S7. Lower expression levels of several flowering repressor genes in *Zmelf3.1 Zmelf3.2* double mutants.

Supplemental Figure S8. ZmLUX1 and ZmLUX2 weakly bind to the *ZmCCT10* promoter.

Supplemental Figure S9. Schematic diagram of retrotransposon insertions in 45 maize inbred lines with high-quality genome assembly.

Supplemental Figure S10. Comparison of the expression of EC target genes in the inbred lines with or without the retrotransposon insertion in *ZmELF3.1*.

Supplemental Figure S11. Positive selection of the NonLTR/*L1* and LTR/*Gypsy* retrotransposons in temperate inbred lines.

Supplemental Table S1. Target genes and their two sgRNA target sequences with PAM of B73 and ZC01.

Supplemental Table S2. Detailed information for the constructs in Figure 5, A and G.

Supplemental Table S3. Mutant or transgenic lines used in this study.

Supplemental Data Set S1. Distribution of LTR/*Gypsy* and NonLTR/*L1* retrotransposons in the 45 inbred lines with high-quality genome assembly.

Supplemental Data Set S2. Genetic variation in the cDNA sequence of *ZmELF3.1* in 160 inbred lines (80 tropical and 80 temperate).

Supplemental Data Set S3. Distribution of LTR/*Gypsy* and NonLTR/*L1* retrotransposons in 415 inbred lines (196 tropical lines and 219 temperate lines).

Supplemental Data Set S4. Distribution of LTR/*Gypsy* and NonLTR/*L1* retrotransposons in 72 teosinte accessions.

Supplemental Data Set S5. Distribution of LTR/*Gypsy* and NonLTR/*L1* retrotransposons in 327 modern temperate maize breeding inbred lines.

Supplemental Data Set S6. Distribution of LTR/Gypsy and NonLTR/*L1* retrotransposons in 1,008 landrace accessions native to the Americas.

Supplemental Data Set S7. Amino acid sequences of ZmELF3.1 in 160 inbred lines (80 tropical and 80 temperate).

Supplemental Data Set S8. Primers used in this study.

Supplemental File S1. Alignment of ELF3 proteins in fas format.

Supplemental File S2. Phylogenetic tree of ELF3 proteins in Newick format.

Supplemental File S3. Alignment of ELF4 proteins in fas format.

Supplemental File S4. Phylogenetic tree of ELF4 proteins in Newick format.

Supplemental File S5. Alignment of LUX proteins in fas format.

Supplemental File S6. Phylogenetic tree of LUX proteins in Newick format.

Funding

This work was supported by the National Key R&D program of China (grant no. 2021YFF1000301), the National Natural Science Foundation of China (32022065, 31921004, and 31871639), the Major Program of Guangdong Basic and Applied Research (2019B030302006), the Agricultural Science and Technology Innovation Program of Chinese

Academy of Agricultural Sciences, and a project from Hainan Yazhou Bay Seed Lab (B21HJ8101).

Conflict of interest statement. The authors declare no competing interests.

References

Bailey TL, Williams N, Misleh C, Li W (2006) MEME: discovering and analyzing DNA and protein sequence motifs. Nucleic Acids Res **34**: W369–W373

Barrett JC, Fry B, Maller J, Daly MJ (2004) Haploview: analysis and visualization of LD and haplotype maps. Bioinformatics **21**: 263–265

Beales J, Turner A, Griffiths S, Snape JW, Laurie DA (2007) A *pseudo-response regulator* is misexpressed in the photoperiod insensitive *Ppd-D1a* mutant of wheat (*Triticum aestivum* L.). Theor Appl Genet **115**: 721–733

Bouchet S, Servin B, Bertin P, Madur D, Combes V, Dumas F, Brunel D, Laborde J, Charcosset A, Nicolas S (2013) Adaptation of maize to temperate climates: mid-density genome-wide association genetics and diversity patterns reveal key genomic regions, with a major contribution of the *Vgt2* (*ZCN8*) locus. PLoS One **8**: e71377

Bradbury PJ, Zhang Z, Kroon DE, Casstevens TM, Ramdoss Y, Buckler ES (2007) TASSEL: software for association mapping of complex traits in diverse samples. Bioinformatics **23**: 2633–2635

Brady SM, Burow M, Busch W, Carlborg Ö, Denby KJ, Glazebrook J, Hamilton ES, Harmer SL, Haswell ES, Maloof JN, et al. (2015) Reassess the *t* test: interact with all your data via ANOVA. Plant Cell **27**: 2088–2094

Bu T, Lu S, Wang K, Dong L, Li S, Xie Q, Xu X, Cheng Q, Chen L, Fang C, et al. (2021) A critical role of the soybean evening complex in the control of photoperiod sensitivity and adaptation. Proc Natl Acad Sci USA **118**: e2010241118

Buckler ES, Holland JB, Bradbury PJ, Acharya CB, Brown PJ, Browne C, Ersoz E, Flint-Garcia S, Garcia A, Glaubitz JC, et al. (2009) The genetic architecture of maize flowering time. Science **325**: 714–718

Cai Z, Zhang Y, Tang W, Chen X, Lin C, Liu Y, Ye Y, Wu W, Duan Y (2022) LUX ARRHYTHMO interacts with ELF3a and ELF4a to coordinate vegetative growth and photoperiodic flowering in irce. Front Plant Sci **13**: 853042

Campoli C, Pankin A, Drosse B, Casao CM, Davis SJ, von Korff M (2013) *HvLUX1* is a candidate gene underlying the *early maturity 10* locus in barley: phylogeny, diversity, and interactions with the circadian clock and photoperiodic pathways. New Phytol **199**: 1045–1059

Castelletti S, Tuberosa R, Pindo M, Salvi S (2014) A MITE transposon insertion is associated with differential methylation at the maize flowering time QTL Vgt1. G3 (Bethesda, MD) **4**: 805–812

Chardon F, Virlon B, Moreau L, Falque M, Joets J, Decousset L, Murigneux A, Charcosset A (2004) Genetic architecture of flowering time in maize as inferred from quantitative trait loci meta-analysis and synteny conservation with the rice genome. Genetics **168**: 2169–2185

Chen H, Zou Y, Shang Y, Lin H, Wang Y, Cai R, Tang X, Zhou J (2008) Firefly luciferase complementation imaging assay for protein-protein interactions in plants. Plant Physiol **146**: 368–376

Chow BY, Helfer A, Nusinow DA, Kay SA (2012) ELF3 recruitment to the *PRR9* promoter requires other evening complex members in the *Arabidopsis* circadian clock. Plant Signal Behav **7**: 170–173

Clough SJ, Bent AF (1998) Floral dip: a simplified method for *Agrobacterium*-mediated transformation of *Arabidopsis thaliana*. Plant J **16**: 735–743

Doyle MR, Davis SJ, Bastow RM, McWatters HG, Kozma-Bognár L, Nagy F, Millar AJ, Amasino RM (2002) The *ELF4* gene controls circadian rhythms and flowering time in *Arabidopsis thaliana*. Nature **419**: 74–77

Ducrocq S, Madur D, Veyrieras JB, Camus-Kulandaivelu L, Kloiber-Maitz M, Presterl T, Ouzunova M, Manicacci D, Charcosset A (2008) Key impact of *Vgt1* on flowering time adaptation in maize: evidence from association mapping and ecogeographical information. Genetics **178**: 2433–2437

Edgar RC (2004) MUSCLE: multiple sequnce alignment with high accuracy and high throughput. Nucleic Acids Res **32**: 1792–1797

FAO (2021) Food and Agriculture Organization of the United Nations Agriculture Databases (FAO). http://faostat.fao.org/

Faure S, Turner AS, Gruszka D, Christodoulou V, Davis SJ, von Korff M, Laurie DA (2012) Mutation at the circadian clock gene *EARLY MATURITY 8* adapts domesticated barley (*Hordeum vulgare*) to short growing seasons. Proc Natl Acad Sci USA **109**: 8328–8333

Flint J, Brown PJ, Upadyayula N, Mahone GS, Tian F, Bradbury PJ, Myles S, Holland JB, Flint-Garcia S, McMullen MD, et al. (2011) Distinct genetic architectures for male and female inflorescence traits of maize. PLoS Genet **7**: e1002383

Ford B, Deng W, Clausen J, Oliver S, Boden S, Hemming M, Trevaskis B (2016) Barley (Hordeum vulgare) circadian clock genes can respond rapidly to temperature in an EARLY FLOWERING 3-dependent manner. J Exp Bot **67**: 5517–5528

Guo L, Wang X, Zhao M, Huang C, Li C, Li D, Yang CJ, York AM, Xue W, Xu G, et al. (2018) Stepwise cis-regulatory changes in *ZCN8* contribute to maize flowering-time adaptation. Curr Biol **28**: 3005–3015

Haberer G, Kamal N, Bauer E, Gundlach H, Fischer I, Seidel MA, Spannagl M, Marcon C, Ruban A, Urbany C, et al. (2020) European maize genomes highlight intraspecies variation in repeat and gene content. Nat Genet **52**: 950–957

Hazen SP, Schultz TF, Pruneda-Paz JL, Borevitz JO, Ecker JR, Kay SA (2005) *LUX ARRHYTHMO* encodes a Myb domain protein essential for circadian rhythms. Proc Natl Acad Sci USA **102**: 10387–10392

Hellens RP, Allan AC, Friel EN, Bolitho K, Grafton K, Templeton MD, Karunairetnam S, Gleave AP, Laing WA (2005) Transient expression vectors for functional genomics, quantification of promoter activity and RNA silencing in plants. Plant Methods **1**: 13

Hicks KA, Millar AJ, Carré IA, Somers DE, Straume M, Meeks-Wagner DR, Kay SA (1996) Conditional circadian dysfunction of the *Arabidopsis early-flowering 3* mutant. Science **274**: 790–792

Hsu PY, Harmer SL (2014) Wheels within wheels: the plant circadian system. Trends Plant Sci **19**: 240–249

Huang C, Sun H, Xu D, Chen Q, Liang Y, Wang X, Xu G, Tian J, Wang C, Li D, et al. (2018) *ZmCCT9* enhances maize adaptation to higher latitudes. Proc Natl Acad Sci USA **115**: 334–341

Hufford MB, Seetharam AS, Woodhouse MR, Chougule KM, Ou S, Liu J, Ricci WA, Guo T, Olson A, Qiu Y, et al. (2021) De novo assembly, annotation, and comparative analysis of 26 diverse maize genomes. Science **373**: 655–662

Hung HY, Shannon LM, Tian F, Bradbury PJ, Chen C, Flint-Garcia SA, McMullen MD, Ware D, Buckler ES, Doebley JF, et al. (2012) *ZmCCT* and the genetic basis of day-length adaptation underlying the postdomestication spread of maize. Proc Natl Acad Sci USA **109**: E1913–1921

Ishida Y, Hiei Y, Komari T (2007) Agrobacterium-mediated transformation of maize. Nat Protoc **2**: 1614–1621

Jiang Y, Yang C, Huang S, Xie F, Xu Y, Liu C, Li L (2019) The ELF3-PIF7 interaction mediates the circadian gating of the shade response in *Arabidopsis*. iScience **22**: 288–298

Jiao Y, Peluso P, Shi J, Liang T, Stitzer MC, Wang B, Campbell MS, Stein JC, Wei X, Chin CS, et al. (2017) Improved maize reference genome with single-molecule technologies. Nature **546**: 524–527

Jin M, Liu X, Jia W, Liu H, Li W, Peng Y, Du Y, Wang Y, Yin Y, Zhang X, et al. (2018) *ZmCOL3*, a CCT gene represses flowering in maize by interfering with the circadian clock and activating expression of *ZmCCT*. J Integr Plant Biol **60**: 465–480

Jung JH, Barbosa AD, Hutin S, Kumita JR, Gao M, Derwort D, Silva CS, Lai X, Pierre E, Geng F, et al. (2020) A prion-like domain in ELF3 functions as a thermosensor in *Arabidopsis*. Nature **585**: 256–260

Kumar S, Stecher G, Tamura K (2016) MEGA7: molecular evolutionary genetics analysis version 7.0 for bigger datasets. Mol Biol Evol **33**: 1870–1874

Lancaster AK, Nutter-Upham A, Lindquist S, King OD (2014) PLAAC: a web and command-line application to identify proteins with prion-like amino acid composition. Bioinformatics **30**: 2501–2502

Lazakis CM, Coneva V, Colasanti J (2011) *ZCN8* encodes a potential orthologue of *Arabidopsis* FT florigen that integrates both endogenous and photoperiod flowering signals in maize. J Exp Bot **62**: 4833–4842

Li Q, Wu G, Zhao Y, Wang B, Zhao B, Kong D, Wei H, Chen C, Wang H (2020) CRISPR/Cas9-mediated knockout and overexpression studies reveal a role of maize phytochrome C in regulating flowering time and plant height. Plant Biotechnol J **18**: 2520–2532

Li YX, Li C, Bradbury PJ, Liu X, Lu F, Romay CM, Glaubitz JC, Wu X, Peng B, Shi Y, et al. (2016) Identification of genetic variants associated with maize flowering time using an extremely large multi-genetic background population. Plant J **86**: 391–402

Liang Y, Liu HJ, Yan J, Tian F (2021) Natural variation in crops: realized understanding, continuing promise. Annu Rev Plant Biol **72**: 357–385

Liang Y, Liu Q, Wang X, Huang C, Xu G, Hey S, Lin HY, Li C, Xu D, Wu L, et al. (2018) *ZmMADS69* functions as a flowering activator through the *ZmRap2.7-ZCN 8* regulatory module and contributes to maize flowering time adaptation. New Phytol **221**: 2335–2347

Liew LC, Hecht V, Sussmilch FC, Weller JL (2014) The pea photoperiod response gene *STERILE NODES* is an ortholog of *LUX ARRHYTHMO*. Plant Physiol **165**: 648–657

Lin R, Ding L, Casola C, Ripoll DR, Feschotte C, Wang H (2007) Transposase-derived transcription factors regulate light signaling in *Arabidopsis*. Science **318**: 1302–1305

Liu H, Zhou X, Li Q, Wang L, Xing Y (2020) CCT domain-containing genes in cereal crops: flowering time and beyond. Teor Appl Genet **133**: 1385–1396

Lu S, Zhao X, Hu Y, Liu S, Nan H, Li X, Fang C, Cao D, Shi X, Kong L, et al. (2017) Natural variation at the soybean *J* locus improves adaptation to the tropics and enhances yield. Nat Genet **49**: 773–779

Mascheretti I, Turner K, Brivio RS, Hand A, Colasanti J, Rossi V (2015) Florigen-encoding genes of day-neutral and photoperiod-densitive maize are regulated by different chromatin modifications at the floral transition. Plant Physiol **168**: 1351–1363

Matsubara K, Ogiso-Tanaka E, Hori K, Ebana K, Ando T, Yano M (2012) Natural variation in *Hd17*, a homolog of *Arabidopsis ELF3* that is involved in rice photoperiodic flowering. Plant Cell Physiol **53**: 709–716

Matsuoka Y, Vigouroux Y, Goodman MM, Sanchez GJ, Buckler E, Doebley J (2002) A single domestication for maize shown by multilocus microsatellite genotyping. Proc Natl Acad Sci USA **99**: 6080–6084

McClung CR (2021) Circadian clock components offer targets for crop domestication and improvement. Genes **12**: 374

Meng X, Muszynski MG, Danilevskaya ON (2011) The *FT*-like *ZCN8* gene functions as a floral activator and is involved in photoperiod sensitivity in maize. Plant Cell **23**: 942–960

Mizuno N, Nitta M, Sato K, Nasuda S (2012) A wheat homologue of *PHYTOCLOCK 1* is a candidate gene conferring the early heading phenotype to einkorn wheat. Genes Genet Syst **87**: 357–367

Murakami M, Matsushika A, Ashikari M, Yamashino T, Mizuno T (2005) Circadian-associated rice pseudo response regulators (*Os*PRRs): insight into the control of flowering time. Biosci Biotechnol Biochem **69**: 410–414

Murphy RL, Klein RR, Morishige DT, Brady JA, Rooney WL, Miller FR, Dugas DV, Klein PE, Mullet JE (2011) Coincident light and clock regulation of *pseudoresponse regulator protein 37* (*PRR37*) controls photoperiodic flowering in sorghum. Proc Natl Acad Sci USA **108**: 16469–16474

Nakamichi N, Kita M, Ito S, Yamashino T, Mizuno T (2005) Pseudo-response regulators, PRR9, PRR7 and PRR5, together play essential roles close to the circadian clock of *Arabidopsis thaliana*. Plant Cell Physiol **46**: 686–698

NCGA (2021) National corn growers association, world of corn (NCGA, WOC, 2021). http://www.worldofcorn.com/#us-select-crop-value

Nieto C, López-Salmerón V, Davière JM, Prat S (2015) ELF3-PIF4 interaction regulates plant growth independently of the evening complex. Curr Biol **25**: 187–193

Nusinow DA, Helfer A, Hamilton EE, King JJ, Imaizumi T, Schultz TF, Farré EM, Kay SA (2011) The ELF4-ELF3-LUX complex links the circadian clock to diurnal control of hypocotyl growth. Nature **475**: 398–402

Pin PA, Zhang W, Vogt Sebastian H, Dally N, Büttner B, Schulze-Buxloh G, Jelly Noémie S, Chia Tansy YP, Mutasa-Göttgens ES, Dohm JC, et al. (2012) The role of a *pseudo-response regulator* gene in life cycle adaptation and domestication of beet. Curr Biol **22**: 1095–1101

Raschke A, Ibañez C, Ullrich KK, Anwer MU, Becker S, Glöckner A, Trenner J, Denk K, Saal B, Sun X, et al. (2015) Natural variants of *ELF3* affect thermomorphogenesis by transcriptionally modulating *PIF4*-dependent auxin response genes. BMC Plant Biol **15**: 197

Reed JW, Nagpal P, Bastow RM, Solomon KS, Dowson-Day MJ, Elumalai RP, Millar AJ (2000) Independent action of ELF3 and phyB to control hypocotyl elongation and flowering time. Plant Physiol **122**: 1149–1160

Romero Navarro JA, Willcox M, Burgueño J, Romay C, Swarts K, Trachsel S, Preciado E, Terron A, Delgado HV, et al. (2017) A study of allelic diversity underlying flowering-time adaptation in maize landraces. Nat Genet **49**: 476–480

Saito H, Ogiso-Tanaka E, Okumoto Y, Yoshitake Y, Izumi H, Yokoo T, Matsubara K, Hori K, Yano M, Inoue H, et al. (2012) *Ef7* encodes an ELF3-like protein and promotes rice flowering by negatively regulating the floral repressor gene *Ghd7* under both short- and long-day conditions. Plant Cell Physiol **53**: 717–728

Salome PA, Weigel D, McClung CR (2010) The role of the Arabidopsis morning loop components CCA1, LHY, PRR7, and PRR9 in temperature compensation. Plant Cell **22**: 3650–3661

Salvi S, Sponza G, Morgante M, Tomes D, Niu X, Fengler KA, Meeley R, Ananiev EV, Svitashev S, Bruggemann E, et al. (2007) Conserved noncoding genomic sequences associated with a flowering-time quantitative trait locus in maize. Proc Natl Acad Sci USA **104**: 11376–11381

Schmittgen TD, Livak KJ (2008) Analyzing real-time PCR data by the comparative C_T method. Nat Protoc **3**: 1101–1108

Springer NM, Anderson SN, Andorf CM, Ahern KR, Bai F, Barad O, Barbazuk WB, Bass HW, Baruch K, Ben-Zvi G, et al. (2018) The maize W22 genome provides a foundation for functional genomics and transposon biology. Nat Genet **50**: 1282–1288

Sun H, Wang C, Chen X, Liu H, Huang Y, Li S, Dong Z, Zhao X, Tian F, Jin W (2020) *dlf1* promotes floral transition by directly activating *ZmMADS4* and *ZmMADS67* in the maize shoot apex. New Phytol **228**: 1386–1400

Sun S, Zhou Y, Chen J, Shi J, Zhao H, Zhao H, Song W, Zhang M, Cui Y, Dong X, et al. (2018) Extensive intraspecific gene order and gene structural variations between Mo17 and other maize genomes. Nat Genet **50**: 1289–1295

Swarts K, Gutaker RM, Benz B, Blake M, Bukowski R, Holland J, Kruse-Peeples M, Lepak N, Prim L, Romay MC, et al. (2017) Genomic estimation of complex traits reveals ancient maize adaptation to temperate North America. Science **357**: 512–515

Thornsberry JM, Goodman MM, Doebley J, Kresovich S, Nielsen D, Buckler EST (2001) *Dwarf8* polymorphisms associate with variation in flowering time. Nat Genet **28**: 286–289

Turner A, Beales J, Faure S, Dunford RP, Laurie DA (2005) The *pseudo-response regulatorPpd-H1* provides adaptation to photoperiod in barley. Science **310**: 1031–1034

Undurraga SF, Press MO, Legendre M, Bujdoso N, Bale J, Wang H, Davis SJ, Verstrepen KJ, Queitsch C (2012) Background-dependent effects of polyglutamine variation in the *Arabidopsis* thaliana gene *ELF3*. Proc Natl Acad Sci USA **109**: 19363–19367

Urban A, Neukirchen S, Jaeger KE (1997) A rapid and efficient method for site-directed mutagenesis using one-step overlap extension PCR. Nucleic Acids Res **25**: 2227–2228

Walter M, Chaban C, Schütze K, Batistic O, Weckermann K, Näke C, Blazevic D, Grefen C, Schumacher K, Oecking C, et al. (2004) Visualization of protein interactions in living plant cells using bimolecular fluorescence complementation. Plant J **40**: 428–438

Wang B, Lin Z, Li X, Zhao Y, Zhao B, Wu G, Ma X, Wang H, Xie Y, Li Q, Song G, et al. (2020) Genome-wide selection and genetic improvement during modern maize breeding. Nat Genet **52**: 565–571

Wang B, Hou M, Shi J, Ku L, Song W, Li C, Ning Q, Li X, Li C, Zhao B, et al. (2022) *De novo* assembly and analyses of twelve founder inbred lines provide genomic insights into heterotic groups and heterosis of maize. Nat Genet Under review

Weller JL, Liew LC, Hecht VF, Rajandran V, Laurie RE, Ridge S, Wenden B, Vander Schoor JK, Jaminon O, Blassiau C, et al. (2012) A conserved molecular basis for photoperiod adaptation in two temperate legumes. Proc Natl Acad Sci USA **109**: 21158–21163

Wydro M, Kozubek E, Lehmann P (2006) Optimization of transient *Agrobacterium*-mediated gene expression system in leaves of *Nicotiana benthamiana*. Acta Biochim Pol **53**: 289–298

Xiao C, Chen F, Yu X, Lin C, Fu YF (2009) Over-expression of an AT-hook gene, *AHL22*, delays flowering and inhibits the elongation of the hypocotyl in *Arabidopsis thaliana*. Plant Mol Biol **71**: 39–50

Xie Y, Liu Y, Ma M, Zhou Q, Zhao Y, Zhao B, Wang B, Wei H, Wang H (2020) Arabidopsis FHY3 and FAR1 integrate light and strigolactone signaling to regulate branching. Nat Commun **11**: 1955

Yang N, Lu Y, Yang X, Huang J, Zhou Y, Ali F, Wen W, Liu J, Li J, Yan J (2014) Genome wide association studies using a new nonparametric model reveal the genetic architecture of 17 gronomic traits in an enlarged maize association panel. PLoS Genet **10**: e1004573

Yang Q, Li Z, Li W, Ku L, Wang C, Ye J, Li K, Yang N, Li Y, Zhong T, et al. (2013) CACTA-like transposable element in *ZmCCT* attenuated photoperiod sensitivity and accelerated the postdomestication spread of maize. Proc Natl Acad Sci USA **110**: 16969–16974

Yang X, Baliji S, Buchmann RC, Wang H, Lindbo JA, Sunter G, Bisaro DM (2007) Functional modulation of the geminivirus AL2 transcription factor and silencing suppressor by self-interaction. J Virol **81**: 11972–11981

Yu J, Pressoir G, Briggs WH, Vroh Bi I, Yamasaki M, Doebley JF, McMullen MD, Gaut BS, Nielsen DM, Holland JB, et al. (2005) A unified mixed-model method for association mapping that accounts for multiple levels of relatedness. Nat Genet **38**: 203–208

Zagotta MT, Hicks KA, Jacobs CI, Young JC, Hangarter RP, Meeks-Wagner DR (1996) The *Arabidopsis ELF3* gene regulates vegetative photomorphogenesis and the photoperiodic induction of flowering. Plant J **10**: 691–702

Zakhrabekova S, Gough SP, Braumann I, Müller AH, Lundqvist J, Ahmann K, Dockter C, Matyszczak I, Kurowska M, Druka A, et al. (2012) Induced mutations in circadian clock regulator *Mat-a* facilitated short-season adaptation and range extension in cultivated barley. Proc Natl Acad Sci USA **109**: 4326–4331

Zhao J, Huang X, Ouyang X, Chen W, Du A, Zhu L, Wang S, Deng X, Li S (2012) *OsELF3-1*, an ortholog of *Arabidopsisearly flowering* 3, regulates rice circadian rhythm and photoperiodic flowering. PLoS One **7**: e43705

Zhao Y, Zhang C, Liu W, Gao W, Liu C, Song G, Li W, Mao L, Chen B, Xu Y, et al. (2016) An alternative strategy for targeted gene replacement in plants using a dual-sgRNA/Cas9 design. Sci Rep **6**: 23890

Zhu C, Peng Q, Fu D, Zhuang D, Yu Y, Duan M, Xie W, Cai Y, Ouyang Y, Lian X, et al. (2018) The E3 ubiquitin ligase HAF1 modulates circadian accumulation of EARLY FLOWERING3 to control heading date in rice under long-day conditions. Plant Cell **30**: 2352–2367

Zuker M (2003) Mfold web server for nucleic acid folding and hybridization prediction. Nucleic Acids Res **31**: 3406–3415